School of Technology and Experimental Sciences

Department of Inorganic and Organic Chemistry

Organic Molecular Nanomaterials with Biomedical Applications group

SYNTHESIS OF NEW CATIONIC BOLAAMPHIPHILES DERIVED FROM L-CYSTINE

Author

Mireia Mercé Moya

Supervisor

Juan Felipe Miravet Celades

Bachelor's Thesis

Castelló de la Plana, July 2023

ABBREVIATIONS

ACN	Acetonitrile
BBr_3	Boron tribromide
Boc	Tert-butyloxycarbonyl
Boc_2O	Di-tert-butyl dicarbonate
CAC	Critical Aggregation Concentration
$CDCl_3$	Deuterated chloroform
CH_2Cl_2	Dichloromethane
CH_3I	Iodomethane
$CHCl_3$	Chloroform
CMC	Critical Micellar Concentration
CPC	Cetylpyridinium chloride
CTAB	Cetyltrimethylammonium bromide
DCC	N,N'-Dicyclohexylcarbodiimide
DIC	N,N'-Diisopropylcarbodiimide
DiOC6(3)	3,30-dihexyloxacarbocyanine iodide
DNA	Deoxyribonucleic acid
DMF	N,N-Dimethylformamide
DMSO-d_6	Deuterated dimethyl sulfoxide
DOTAP	1,2-Dioleoyl-3-trimethylammonium-propane chloride
DOTMA	N-[1-(2,3-dioleyloxy)propyl]-NNN-trimethylammonium chloride
DTT	Dithiothreitol
eq.	Equivalent
EPR	Enhanced Permeability and Retention
ESI-TOF	Electrospray Ionization Time of Flight
FDA	United States Food and Drug Administration
GSH	Glutathione
HB	Hypericin
HBr	Hydrobromic acid

HBTU	2-(1H-Benzotriazole-1-yl)-1,1,3,3-tetramethylaminium hexafluorophosphate
HCl	Hydrochloric acid
HCTU	O-(1H-6-Chlorobenzotriazole-1-yl)-1,1,3,3-tetramethyluronium hexafluorophosphate
HF	Hydrofluoric acid
HRM	High Resolution Mass Spectrometry
HT-29	Human colorectal adenocarcinoma cells
K_2CO_3	Potassium carbonate
m/z	Mass/charge
MeOH	Methanol
$MeSO_3H$	Methanesulphonic acid
MHz	Megahertz
NAC	N-acetylcysteine
NaOH	Sodium hydroxide
NMR	Nuclear Magnetic Resonance
N_2	Nitrogen
NR	Nile Red
PDT	Photodynamic therapy
PEG	Polyethylene glycol
PLD	Pegylated Liposomal Doxorubicin
PNPA	p-nitrophenyl acetate
PTX	Paclitaxel
RB	Rose Bengal
RNA	Ribonucleic acid
$SOCl_2$	Thionyl chloride
TEM	Transmission Electron Mycroscopy
TFA	Trifluoroacetic acid
TBTU	2-(1H-Benzotriazole-1-yl)-1,1,3,3-tetramethylaminium tetrafluoroborate
TCEP	tris(2-carboxyethyl)phosphine hydrochloride
TMS-Cl	Trimethylsilyl chloride
Z/Cbz	Benzyloxycarbonyl

INDEX

Introduction

1.1 Cationic vesicles

1.1.1 Vesicles, liposomes and micelles

Vesicles are a general term to describe any structure enclosed by a lipid membrane and can be of natural origin, found within cells and organelles, or of artificial origin, such as giant liposomes. In this context, liposomes stand out as one of the most studied and used artificial vesicles in drug delivery systems (DDSs) due to their biocompatibility, stability, ease of synthesis, high drug-loading efficiency and high bioavailability.

Liposomes, discovered in the 1960s by Bergham, are spherical vesicles formed by one or more phospholipid bilayers, which are amphiphilic molecules that have a hydrophilic head and a hydrophobic tail. These structures spontaneously form when in contact with and aqueous medium, where the hydrophilic parts orient towards the exterior and the hydrophobic parts towards the interior, thus forming a lipid bilayer that encloses an aqueous compartment inside. The diameter of typical liposomes ranges from 50 to 500 nm, however, when used for drug delivery purposes, the size of these vesicles typically ranges from 50 to 150 nm.[1] [2]

In the laboratory, there are various techniques to produce liposomes and their structure can vary. Unilamellar liposomes can be obtained, which consist of a single lipid layer. It is also possible to generate multilamellar liposomes, which are composed of multiple lipid layers surrounding the internal aqueous compartment. Additionally, there are multivesicular liposomes, where smaller vesicles are contained within a single external lipid layer.

[1] Nsairat. H., Khater, D., Sayed, U., Odeh, F., Bawab, A. A., & Alshaer, W. (2022). "Liposomes: structure, composition, types and clinical applications." *Heliyon*, 8(5), e09394.

[2] Van Der Koog, L., Gandek, T. B. & Nagelkerke, A. (2021) "Liposomes and Extracellular Vesicles as Drug Delivery Systems: A Comparison of Composition, Pharmacokinetics, and Functionalization." *Advanced Healthcare Materials*, 11(5), 2100639.

On the other hand, when it comes to single-chain amphiphilic molecules, a different type of aggregates known as micelles form upon contact with and aqueous medium. The concentration at which this phenomenon occurs is referred to as critical micelle concentration (CMC). Similar to liposomes, micelles are composed of hydrophobic chains that orient towards the interior, and an external hydrophilic layer formed by the polar heads of the molecules, which orient towards the exterior and are in contact with the surrounding aqueous medium.

The interior of micelles is entirely non-polar (unlike liposomes, which have an aqueous core), making it suitable for dissolving and transporting non-polar or hydrophobic compounds in aqueous environments. This property is particularly useful in drug delivery. [3]

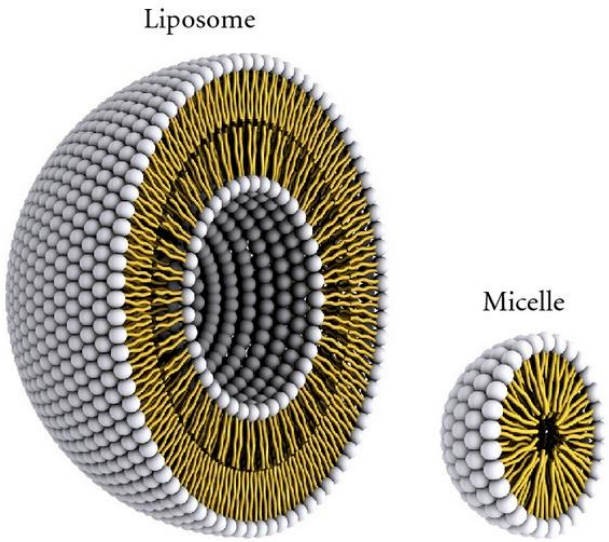

Figure 1.1: Schematic representation of the structure of a liposome and a micelle, respectively. [4]

[3] Furton, K. G. & Norelus, A. (1993). "Determining the critical micelle concentration of aqueous surfactant solutions: Using a novel colorimetric method." *Journal of Chemical Education*, 70(3), 254.

[4] Bitounis, D., Fanciullino, R., Iliadis, A. & Ciccolini, J. (2012). "Optimizing Druggability through Liposomal Formulations: New Approaches to an Old Concept." *ISRN Pharmaceutics (Print), 2012*, 1-11.

1.1.2. Vesicles in drug delivery

Traditional drug administration has been a fundamental tool in the treatment of various diseases, but it often presents limitations in terms of efficacy and side effects. However, drug delivery systems (DDSs) offer promising potential to enhance pharmacological therapy. These systems involve the use of nanocarriers to deliver drugs more effectively to their site of action, prolong their residence time in target cells and minimize unwanted side effects.

To achieve this, nanoparticles of different material such as ceramics, polymers, metals and lipids are employed. These nanoparticles, ranging in size from a few nanometers to several hundreds of nanometers, offer unique properties that can be leveraged to enhance the characteristics of traditional treatments. Among the most investigated and utilized nanocarriers are liposomes due to their high biocompatibility, biodegradability and low immunogenicity. These vesicles have shown to improve drug solubility and controlled distribution and they can also modify their surface to achieve targeted, prolonged and sustained release. The structure of liposomes allows for the accommodation of cargo both in their lipid bilayer (hydrophobic substances) and in their aqueous core (hydrophilic substances).

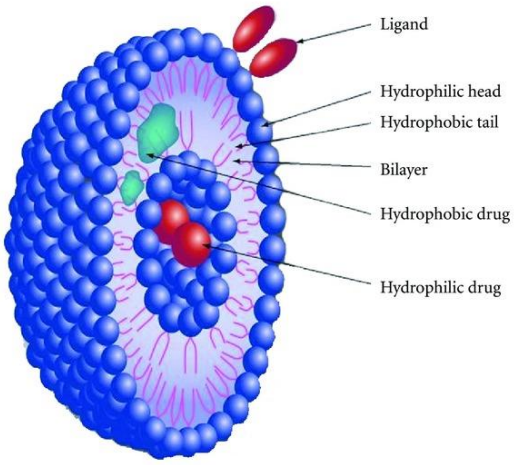

Figure 1.2: Schematic representation of the locations where drugs can be stored in a unilamellar liposome. [5]

[5] Christoforidis, J. B., Chang, S., Jiang, A., Wang, J. & Cebulla, C. M. (2012). "Intravitreal Devices for the Treatment of Vitreous Inflammation." *Mediators of Inflammation*, 2012, 1-8.

Pegylated liposomal doxorubicin (PLD) was the first nanomedicine approved for cancer treatment in 1994 for clinical use by the United States Food and Drug Administration (FDA). This advanced form of doxorubicin is characterized by being encapsulated in liposomes coated with polyethylene glycol (PEG).

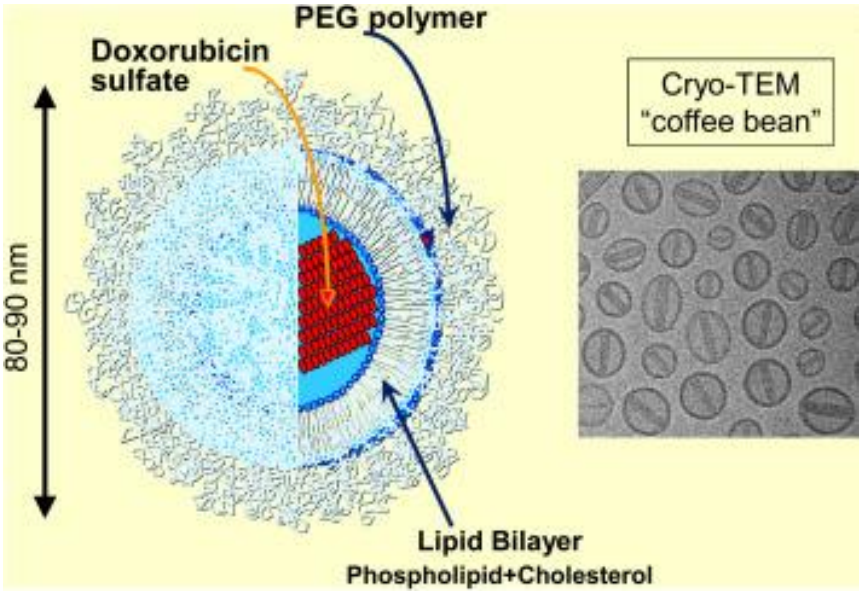

Figure 1.3: On the left, schematic representation of doxorubicin encapsulated by a liposome coated with the polymer PEG. On the right, an image obtained from PLD using CryoTEM, showing a rod-shaped precipitate (doxorubicin sulfate).[6]

PLD has been shown to be effective in the treatment of various types of cancer, such as HIV-related Kaposi sarcoma, advanced ovarian cancer, metastatic breast cancer and multiple myeloma. It also offers several advantages over conventional doxorubicin. The liposomes coated with PEG provide greater stability in the bloodstream and are less detected by the mononuclear phagocytic system, prolonging their circulation time and accumulation in the tumor. Furthermore, it significantly reduces the cardiotoxicity associated with conventional doxorubicin.

When administering PLD, liposomes preferentially accumulate in the tumor region due to a phenomenon called Enhanced Permeability and Retention (EPR) effect. This effect is characterized by increased permeability of tumor blood vessels and prolonged retention of nanoparticles in the tumor tissue (***Figure 1.4,*** *1*). Once the liposomes extravasate into the tumor interstitial fluid, they release doxorubicin, which then diffuses into nearby tumor cells (***Figure 1.4,*** *2*). Upon internalization of PDL liposomes by tumor cells (TC) or macrophages (TAM), their intracellular trafficking is limited to endosomes and lysosomes, compartments responsible for processing and degrading molecules (***Figure 1.4,*** *3*). Finally, doxorubicin is released from the endosomes or lysosomes and enters the nucleus of the tumor cell where it exerts its therapeutic effect (***Figure 1.4,*** *4*).[6]

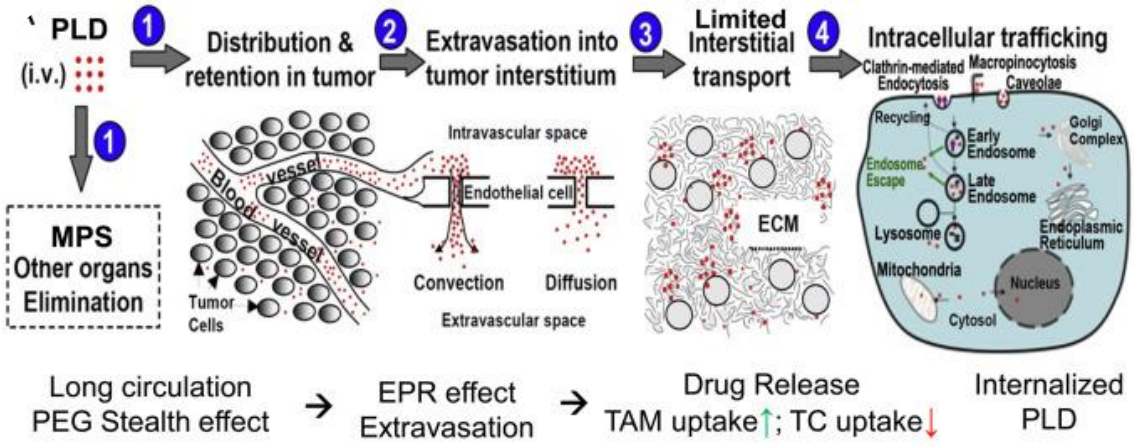

Figure 1.4: *Delivery of PDL to the tumor and release and penetration of doxorubicin into tumor cells.*[6]

[6] Gabizon, A., Patil, Y. & La-Beck, N. M. (2016). "New insights and evolving role of pegylated liposomal doxorubicin in cancer therapy." *Drug Resistance Updates*, 29, 90-106.

1.1.3. Cationic vesicles as nanocarriers

Cationic liposomes (CLs) are a variant of liposomes that have a positive charge on their surface, enabling them to interact with negatively charged molecules. In recent years, extensive research has been conducted on the use of cationic liposomes as vehicles for the delivery of nucleic acids (NAs) for therapeutic purposes. Breakthroughs in this field were pioneered by Philip Felgner and his team of collaborators. In their investigations, they demonstrated that positively charged CLs can form complexes with negatively charged NAs and bind to the anionic sulfate groups of proteoglycans present on the cell surface of mammalian cells. This interaction facilitated the uptake of nucleic acids by the cells and allowed for the expression of the administrated DNA and RNA.

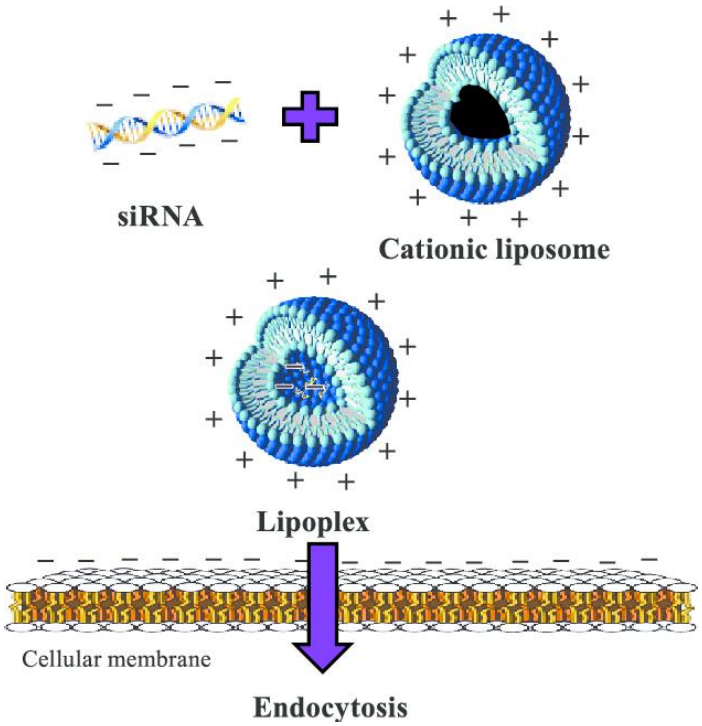

Figure 1.5: Pictorial representation of the interaction between a cationic liposome and an anionic siRNA, resulting in the formation of a lipoplex that interacts with the negatively charged cell membrane. This leads to improved delivery into cells through endocytosis.[7]

[7] Youngren-Ortiz, S. R., Gandhi, N., España-Serrano, L. & Chougule, M. B. (2017). "Aerosol Delivery of siRNA to the Lungs. Part 2: Nanocarrier-based Delivery Systems." *Kona Powder and Particle Journal, 34(0)*, 44-69.

Specifically, one of the research studies conducted by Felgner focused on the technique of cationic liposome-mediated RNA transfection. In particular, the researchers in this study employed a cationic lipid called N-[1-(2,3-dioleyloxy)propyl]-NNN-trimethylammonium chloride (DOTMA) to encapsulate RNA molecules and deliver them efficiently to cells. The results of this study demonstrated that cationic liposomes, specifically those formed by DOTMA, are efficient for RNA transfection in different types of cells.[8]

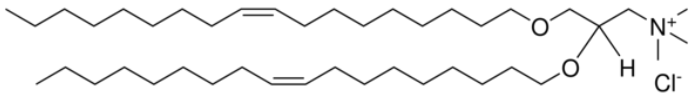

Figure 1.6: The structure of DOTMA used in Felgner's study for the formation of cationic liposomes.[8]

There are different structures of cationic lipids, some of which are shown in *Figure 1.7*:

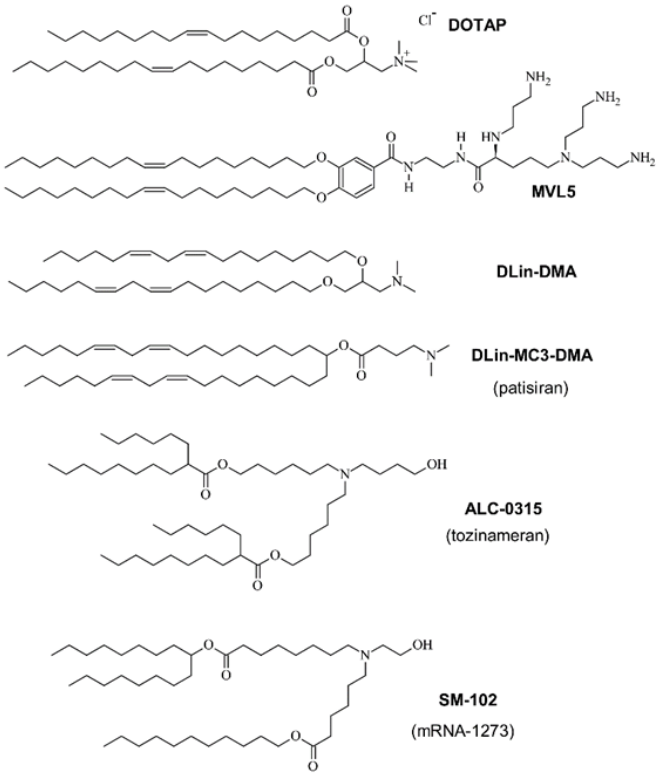

Figure 1.7: Different structures of cationic lipids used in cationic lipid-nucleic acid (CL-NA) nanoparticle formulations.[9]

[8] Malone, R. W., Felgner, P. L. & Verma, I. M. (1989). "Cationic liposome-mediated RNA transfection." *Proceedings of the National Academy of Sciences, 86(16)*, 6077-6081.

In addition to nucleic acid delivery, cationic liposomes have also been extensively studied as vehicles for delivering hydrophobic drugs used in cancer treatment. Due to their hydrophobic nature, these drugs are incorporated within the lipid bilayer of liposomes (hydrophobic environment). This characteristic allows the drugs to remain associated with the lipid membranes when combined with nucleic acids, offering the possibility of dual-action combined therapies.

For example, paclitaxel is one of the most used chemotherapy drugs for treating various types of cancer, but it has the drawback of being hydrophobic. For this reason, it requires carriers for effective delivery. Cationic liposomes have shown the ability to specifically target tumor areas and be readily taken up by cancer cells, making them desirable vectors for hydrophobic drugs that need to penetrate cells to exert their therapeutic effects.[9]

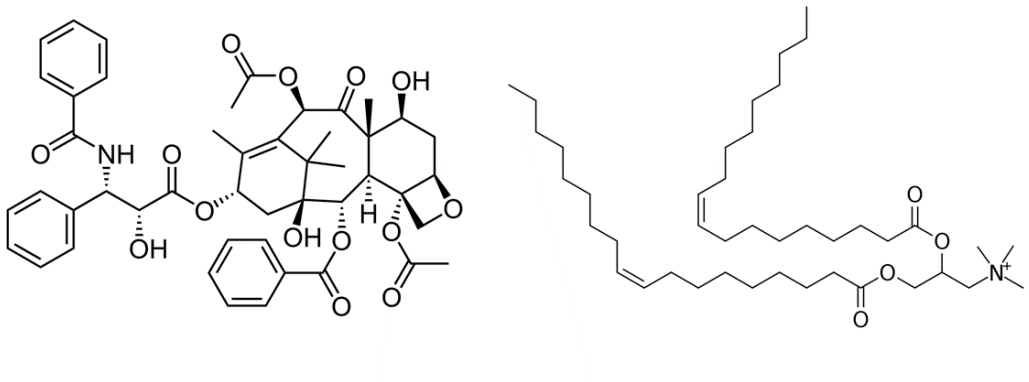

Figure 1.8: On the left, the chemical structure of the drug paclitaxel (PTX). On the right, the structure of the cationic lipid (DOTAP) used to form the cationic liposomes that encapsulate the drug.

[9] Ewert, K. K., Scodeller, P., Simón-Gracia, L., Steffes, V. M., Wonder, E., Teesalu, T. & Safinya, C. R. (2021). "Cationic Liposomes as Vectors for Nucleic Acid and Hydrophobic Drug Therapeutics." *Pharmaceutics, 13(9)*, 1365.

1.1.4. Vesicles from bolaamphiphiles

Bolaamphiphilic molecules are structures consisting of a hydrophobic part, such as and alkyl chain, and two hydrophilic polar units at the ends. These molecules can self-assemble in water, which means they can form ordered and stable structures in an aqueous environment. Unlike conventional liposomes, which have a double-layered lipid membrane, vesicles formed by amphiphilic molecules have a single-layered membrane, providing them with greater thermal stability. In the literature, there are relatively few cationic bolaamphiphilic vesicles that exhibit different polar terminal groups, such as paraquat, trimethylammonium or dequalinium.[10]

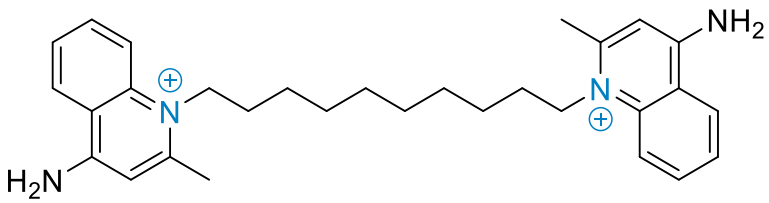

Dequalinium

Figure 1.9: Chemical structure of dequalinium.

Fullerenes, such as [60]fullerene, modified with bolaamphiphilic groups, enable the self-assembly of [60]fullerenes into vesicular structures in the presence of water. These compounds have demonstrated unique and versatile properties that make them attractive for vesicle formation and delivery of therapeutic payloads.[11]

[10] Ana M. Bernal-Martínez, César A. Angulo-Pachón, Francisco Galindo, Juan F. Miravet. (2023). "Reduction-Responsive Cationic Vesicles from Bolaamphiphiles with Ionizable Amino Acid or Dipeptide Polar Heads." (Submitted)

[11] Sano, M., Oishi, K., Ishi-I, T. & Shinkai, S. (2000). "Vesicle Formation and Its Fractal Distribution by Bola-Amphiphilic [60]Fullerene." *Langmuir, 16(8),* 3773-3776.

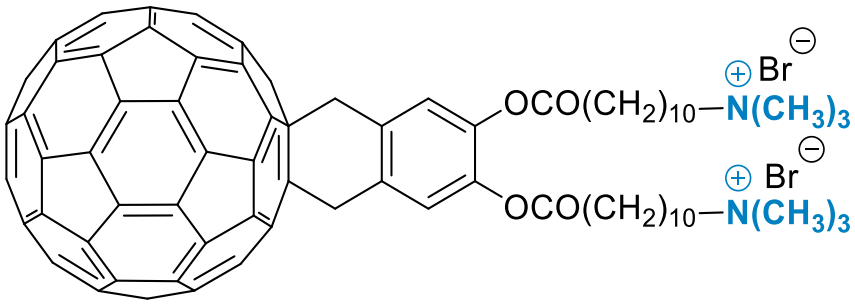

Figure 1.10: *Chemical structure of [60]fullerene with trimethylammonium as terminal groups.*

Furthermore, bolaamphiphilic compounds with acetylcoline groups at the ends have also been studied. The findings of the conducted study demonstrated the formation of cationic vesicles with good stability, as well as exhibiting efficient encapsulation and controlled release of the evaluated therapeutic molecules. Additionally, efficient internalization of the vesicles in different types of cells was observed.[12]

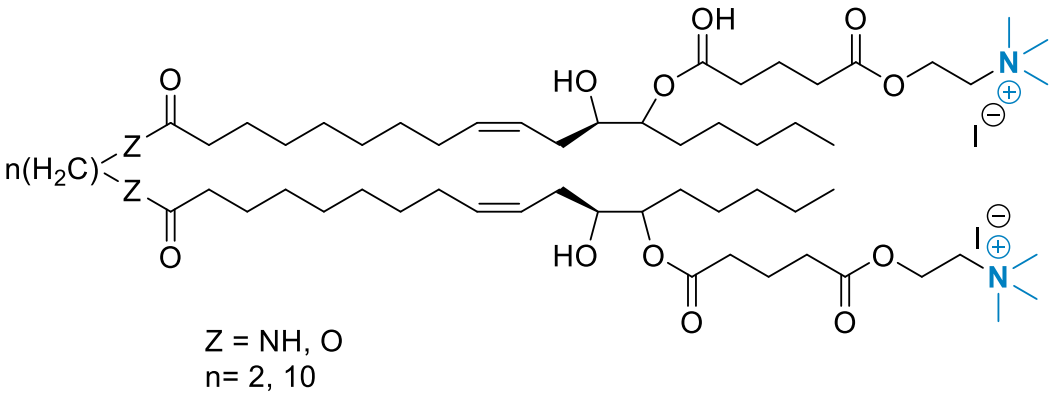

Figure 1.11: *Bolaamphiphiles with acetylcoline groups at the ends.*

These same bolaamphiphiles (***Figure 1.11***), in a separate study, were capable of efficiently encapsulating analgesic peptides and releasing them in the brain, crossing the blood-brain barrier. [13]

[12] Popov, M., Linder, C., Deckelbaum, R. J., Griberg, S., Hansen, I. H., Shaubi, E., Waner, T. & Heldman, E. (**2010**). "Cationic vesicles from novel bolaamphiphilic compounds." *Journal of Liposome Research, 20(2),* 147-159.

[13] Popov, M., Hammad, I. A., Bachar, T., Grinberg, S., Linder, C., Stepensky, D. & Heldman, E. (**2013**). "Delivery of analgesic peptides to the brain by nano-sized bolaamphiphilic vesicles made of monolayer membranes." *European Journal of Pharmaceutics and Biopharmaceutics, 85(3),* 381-389.

1.2 Nanocarriers with disulfide units

In recent decades, nanomaterials containing disulfide bonds have received special attention due to their great potential as drug and gene carriers.

The disulfide bond present in these nanomaterials can remain stable in the bloodstream and extracellular environment, preventing premature drug release and reducing the possibility of systemic toxicities. However, upon entering cancer cells, as exchange reaction occurs between the disulfide bond and the sulfhydryl (-SH) bond of glutathione (GSH), which is highly concentrated in the cytoplasm. This interaction leads to the breaking of the disulfide bond, resulting in the disintegration of the nanocarrier and, consequently, a rapid release of the drug.

Glutathione is a tripeptide composed of three amino acids (glutamate, cysteine and glycine) and acts as an important antioxidant in cells by donating electrons to neutralize free radicals and other reactive species, thereby preventing oxidative damage to cellular structures.

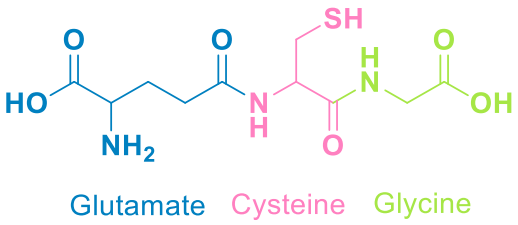

Figure 1.12: *Chemical structure of glutathione (GSH).*

This redox-responsive mechanism has generated great interest in the field of cancer treatment, as the intracellular environment is reducing, with a high concentration of GSH. It is important to note that the concentration of GSH is significantly higher inside cells compared to the extracellular environment and cancer cells have even higher levels of GSH than healthy cells. This characteristic provides a unique opportunity to use nanomaterials containing disulfide bonds as specific drug delivery systems for cancer cells.[14]

[14] Fu, S., Rempson, C. M., Puche, V., Zhao, B., & Zhang, F. (2021). "Construction of disulfide containing redox-responsive polymeric nanomedicine." *Methods, 199*, 67-79.

A type of disulfide-crosslinked micelles has been developed, which are reduction-sensitive and exhibit excellent stability, prolonged blood circulation time and minimal premature drug release.

Figure 1.13: Schematic representation of disulfide-crosslinked micelles formed by the oxidation of the thiolated telodendrimer PEG5k-Cys4-L8-CA8 after self-assembly.[15]

In *Figure 1.13*, it shows how the crosslinked micelles are formed by the oxidation of a thiolated telodendrimer, called PEG5k-Cys4-L8-CA8 (PEG5k is a 5000 molecular weight polyethylene glycol that forms the outer layer of the micelle, Cys4 refers to four cysteine residues and L8-CA8 refers to a dendrimer structure with eight branches, which is the hydrophobic part capable of encapsulating and transporting drugs inside). First, the self-assembly process takes place, where the telodendrimer organizes into micelles. Subsequently, the oxidation of thiol (-SH) groups of the cysteine rediues occurs, leading to disulfide bonds (-S-S-) between the cysteine residues, providing stability and allowing control over drug release.

[15] Li, Y., Xiao, K., Zhu, W., Deng, W. & Lam, K. S. (2014). "Stimuli-responsive cross-linked micelles for on-demand drug delivery against cancers." *Advanced Drug Delivery Reviews, 66,* 58-73.

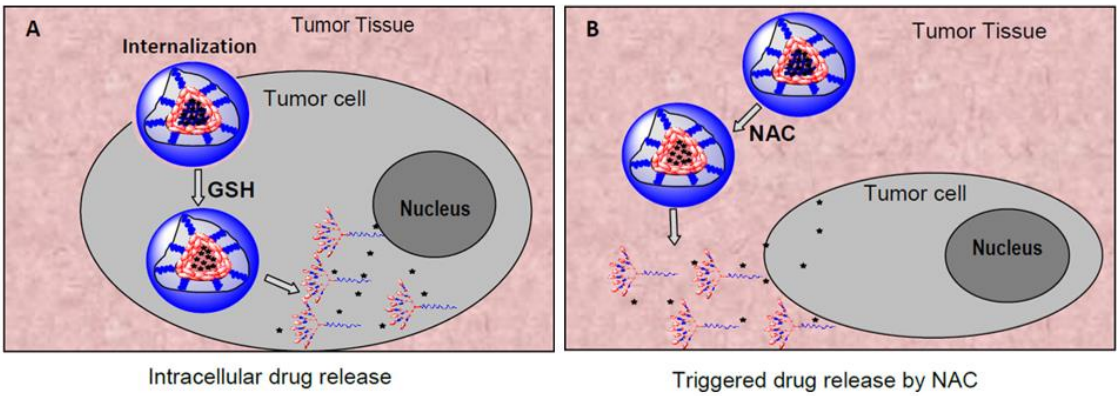

Figure 1.14: Schematic representation of hypothetical mechanisms for controlled drug release by reducing agents (A: GSH. B: NAC) upon accumulation of PTX micelles at tumor sites.[14]

In mechanism A, as PTX micelles accumulate at the tumor site, high levels of GSH present can react with the disulfide bonds and break them, thereby releasing paclitaxel from the micelles for subsequent diffusion into cancer cells. In mechanism B, the breaking of intramicellar disulfide bridges and the consequent drug release also occur, but using a different reducing agent, N-acetylcysteine (NAC).

1.3 Previous work in the group

In recent years, the research group where this bachelor thesis has been carried out, "ORGANANO – Nanomateriales Moleculares Orgánicos con Aplicaciones Biomédicas", has been dedicated to the synthesis of self-assembled molecular nanoparticles that respond to stimuli and the study of their potential biomedical applications.

In a recent study, several bolaamphiphilic compounds were synthesized, containing a central unit derived from cystamine and a terminal unit corresponding to an amino acid or a dipeptide. The selected amino acids (phenylalanine, tryptophan and valine) have hydrophobic and non-ionizable side chains, which promote aggregation in an aqueous medium. These bolaamphiphilic were designed with the aim of forming stable and reduction-sensitive cationic vesicles.

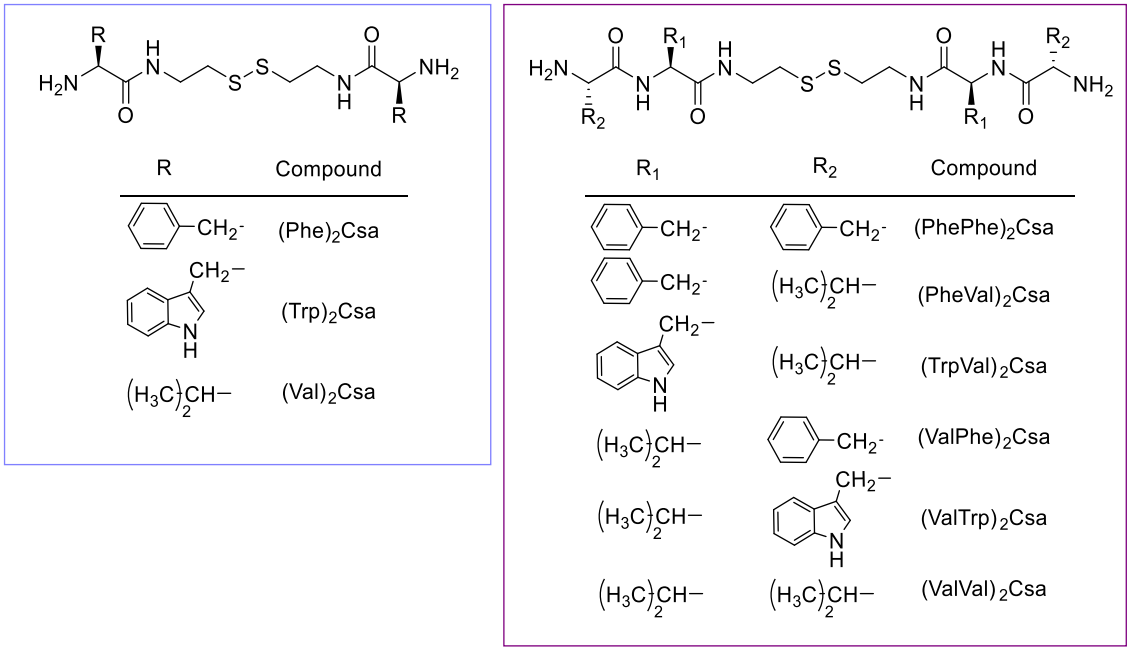

Scheme 1.1: *On the right, the synthesized bolaamphiphilic compunds that have dipeptides as terminal units. On the left, those that have amino acids as terminal units.*

It was observed that among all the synthesized bolaamphiphiles compounds, those that formed cationic vesicles in an aqueous medium were the ones that had dipeptides as terminal units in an acidic environment (pH ≈ 4). However, compounds with individual amino acids were less prone to aggregation.

Dynamic light scattering (DLS) studies allowed the observation of vesicle formation with diameters ranging from approximately 140 to 500 nm. Some of the compounds were also imaged using transmission electron mycroscopy (TEM).

These compounds were sensitive to a reducing environment due to the disulfide bridge present in their structure. The reduction responsiveness was confirmed using ^{1}H-NMR and employing a hydrophobic dye, Nile Red (NR). The uptake of NR by the vesicles causes a drastic change in fluorescence and UV-Vis spectra. Upon the addition of a reducing agent, tris(2-carboxyethyl)phosphine hydrochloride (TCEP), a significant decrease in fluorescence intensity and UV-Vis absorption was observed, indicating vesicle desintegration and NR release.

Therefore, these vesicles demonstrated the ability to encapsulate hydrophobic compunds and release them in reducing environments. Being stable in acidic media, such as the gastric environment, the designed bolaamphiphilic molecules could be used as nanocarriers for gastrointestinal administration, offering a promising alternative for drug delivery. [10]

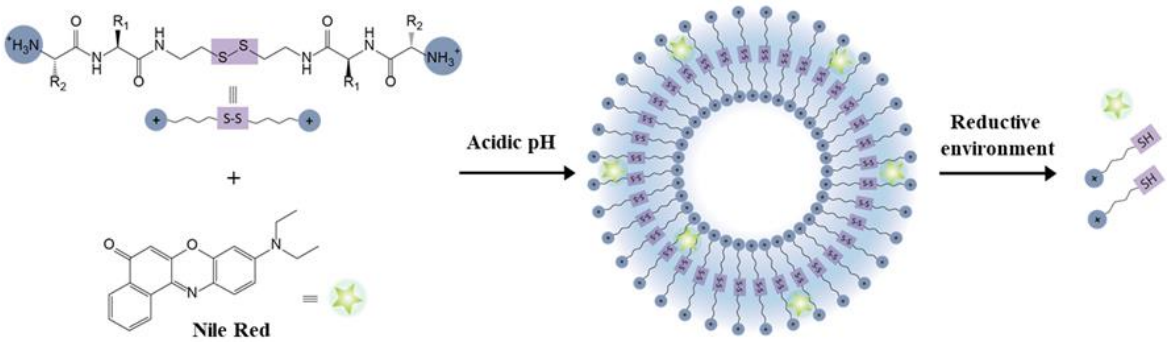

Figure 1.15: Representation of the formation of bolaamphiphiles and the reduction-induced decomposition.[10]

In 2020, two supramolecular hydrogelators (low molecular weight molecules that self-assemble into fibrillar networks that percolate the solvent) were synthesized from L-isoleucine or L-valine, cystamine and succinic or glutaric anhydride amino acids. These hydrogelators contained a central disulfide group sensitive to reducing environments, as well as carboxylic acid terminal units sensitive to pH. It was observed that the gels formed only at a pH below 4, when the hydrogelators were in their neutral form. At higher pH values, ionic species predominated, which, being soluble in water, were unable to form gels.

The responsiveness of the gels to reducing species such as TCEP was evaluated, using the release of the Bromophenol Blue dye as a proof of concept. As expected, upon addition of TCEP, the gels disintegrated and release the dye. Furthermore, insulin was loaded into the gels and it was found that the insulin was protected from degradation in the presence of simulated gastric fluid containing pepsin, a medium that rapidly hydrolyzes free insulin. A change from acidic to neutral pH, as occurs in the gastrointestinal tract, resulted in gel solubilization and the consequent quantitative release of unaltered insulin. This behavior enables the use of hydrogels for oral insulin administration.[16]

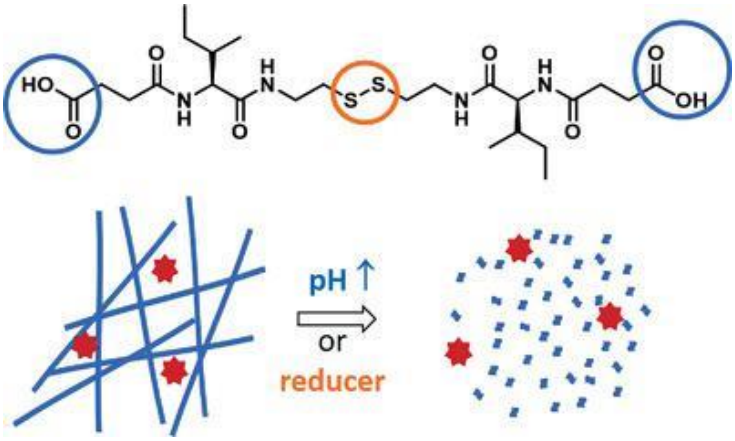

Figure 1.16: *Chemical structure of one of the synthesized hydrogelators (GltValCsa) and pictorial representation of gel dissociation in basic pH or reducing environment.*[16]

[16] Navarro-Barreda, D., Angulo-Pachón, C. A., Bedrina, B., Galindo, F. & Miravet, J. F. (2020). "A Dual Stimuli Responsive Supramolecular Gel Provides Insulin Hydrolysis Protection and Redox-Controlled Release of Actives." *Macromolecular Chemistry and Physics, 221(4),* 1900419.

In 2021, the use of non-polymeric nanogels formed by a low molecular weight hydrogelator was evaluated as nanocarriers capable of transporting both hydrophobic and hydrophilic agents. Specifically, the synthesized non-polymeric nanogels were studied to determine their ability to intracellularly transport two photodynamic therapy (PDT) agents, Rose Bengal (RB) and Hypericin (HB), two photosensitizers with opposing properties that presented challenges in clinical applications. While RB exhibits high polarity and water solubility, HP is poorly polar and poorly soluble in water. It was found that the non-polymeric nanogels provided efficient transport of both agents into human colorectal adenocarcinoma cells (HT-29) and improved PDT efficiency, without significant toxicity in the absence of light, confirming the biocompatibility of the release systems. [17]

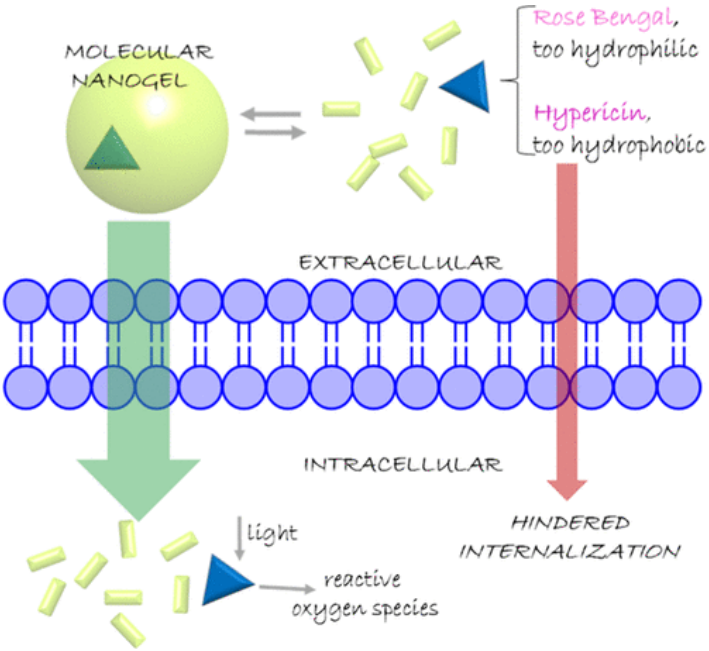

Figure 1.17: Pictorial representation of the use of molecular nanogels as nanocarriers, enabling the entry of RB and HB photosensitizers into cancer cells.[17]

[17] Torres-Martínez, A. C., Bedrina, B., Falomir, E., Marín, M. L. G., Angulo-Pachón, C. A. & Miravet, J. F. (2021). "Non-Polymeric Nanogels as Versatile Nanocarriers: Intracellular Transport of the Photosensitizers Rose Bengal and Hypericin for Photodynamic Therapy." *ACS applied bio materials*, 4(4), 3658-3669.

In the same year, molecular nanoparticles were also prepared in aqueous media using a bolaamphiphile (SucIleCsa) containing a disulfide bond, providing sensitivity to reducing environments. These nanoparticles demonstrated the ability to efficiently load a lipophilic mitochondrial marker, 3,30-dihexyloxacarbocyanine iodide abbreviated as DiOC6(3), which exhibits weak fluorescence in water but becomes highly fluorescent when incorporated into nonpolar environments. The responsiveness of the nanoparticles to reducing agents was confirmed through DLS measurements and ^{1}H-NMR. It was observed that the addition of dithiothreitol (DTT) resulted in the disassembly of the nanoparticles. Similar results were obtained with GSH. Upon investigating the transport of DiOC6(3) in HT-29 cells, it was observed that the use of these nanocarriers significantly improved the uptake of the dye by the cells. An increase in fluorescence upon entering the cells was also observed, which could be related to the disintegration of the nanoparticles (as initially loading the dye into the nanoparticles led to a decrease in fluorescence). The study was also conducted on cells stimulated to produce a higher amount of GSH and increased fluorescence was observed, confirming that the disintegration of the nanoparticles in a reducing environment is a crucial step in the process.

Therefore, these novel molecular nanoparticles can be considered a theranostic tool that achieves both targeted delivery of lipophilic substances and signals high levels of GSH simultaneously.[18]

[18] Navarro-Barreda, D., Bedrina, B. & Miravet, J. F. (2022). "Glutathione-responsive molecular nanoparticles from a dianionic bolaamphiphile and their use as carriers for targeted delivery." *Journal of Colloid and Interface Science*, 608, 2009-2017.

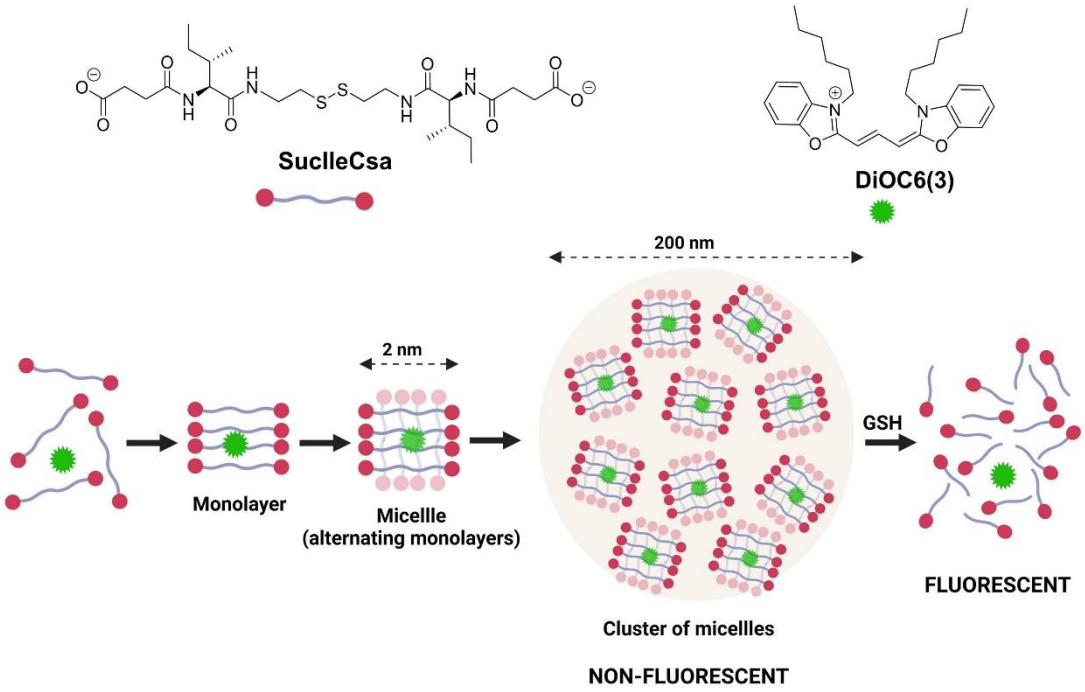

Figure 1.18: Above, the chemical structures of the bolaamphiphile and the lipophilic dye are represented, respectively. Below, the formation of the nanoparticles and their disintegration upon exposure to GSH are depicted, resulting in an increase in the fluorescence of the dye upon release.[18]

In 2023, the formation of nanorods through the co-assembly of cationic surfactants such as cetyltrimethylammonium bromide (CTAB) and cetylpyridinium chloride (CPC), with a cystine derivative sensitive to reducing environments and pendant imidazole groups has been studied. It was found that the nanorods were responsive to the presence of reducing agents, particularly when TCEP was used, leading to their fragmentation. Upon disintegration of the nanostructure, catalytic activity was observed, attributed to the presence of thiol and imidazole functional groups. The resulting molecule after the reductive cleavage could be considered as a mimic of cysteine proteases. The reaction carried out to evaluate the hydrolase-like activity was the hydrolysis of p-nitrophenyl acetate (PNPA).[19]

[19] Navarro-Barreda, D., Angulo-Pachón, C. A., Galindo, F. & Miravet, J. F. (2023). "Reduction-triggered Disassembly of Organic Cationic Nanorods Produces a Cysteine Protease Mimic." *Chemistry: A European Journal*, 29(27).

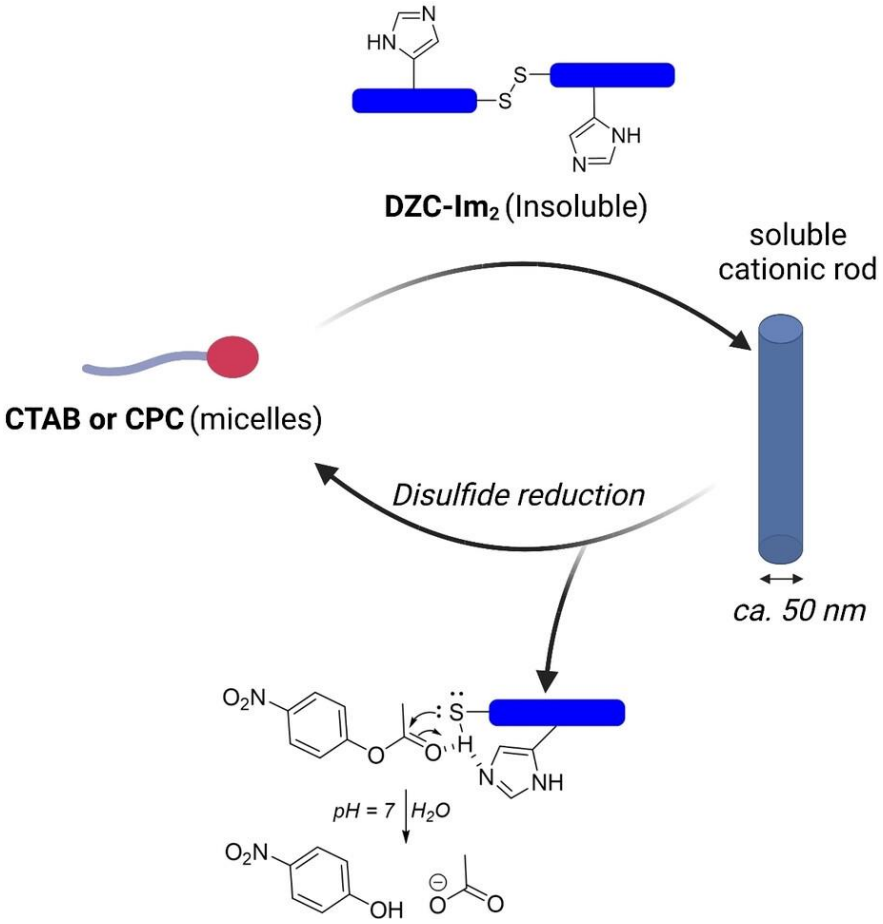

Figure 1.19: Representation of the formation of the nanorod, its reductive dissociation and the studied catalytic process.[19]

Objectives

The stablished objectives are as follows:

1) Synthesize three bolaamphiphilic compounds derived from L-cystine that are pH-independent and sensitive to reducing environments.

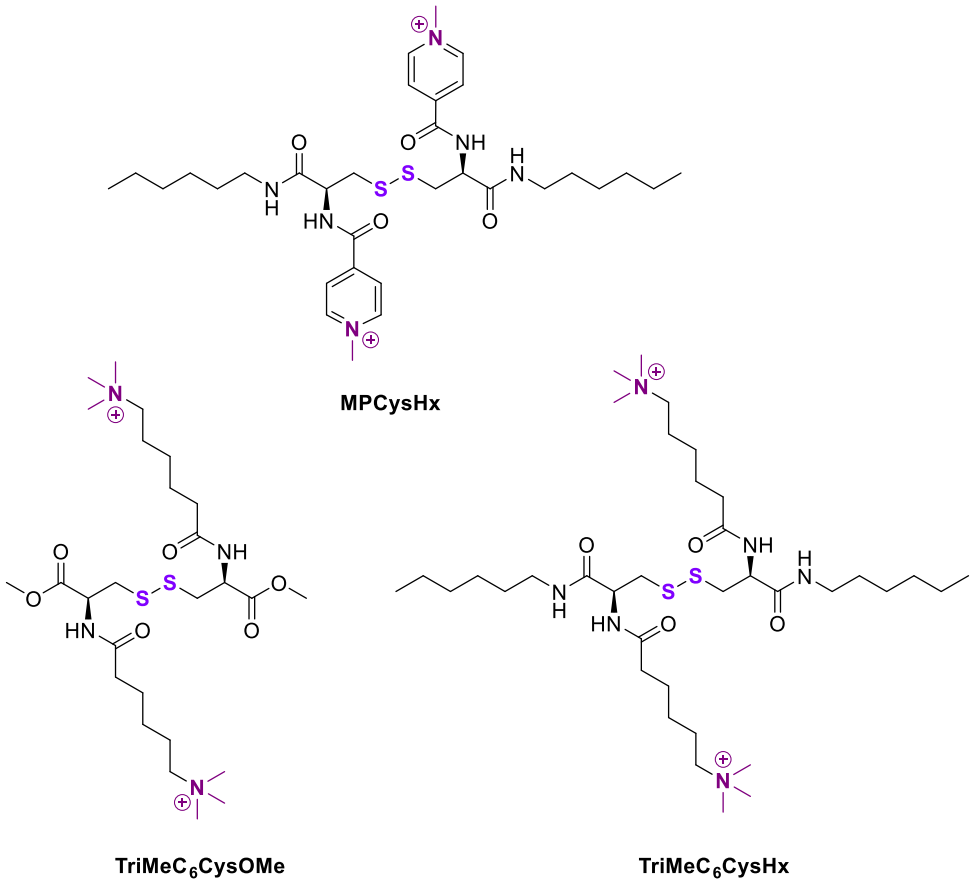

Scheme 2.1: Chemical structure of the three bolaamphiphilic compounds derived from L-cystine.

2) Determine if the synthesized bolaamphiphilic structures can form vesicles in an aqueous medium.
3) Evaluate the incorporation of hydrophobic substrates in the vesicles.
4) Evaluate the reduction-triggered vesicle disassembly of the vesicles and consequent cargo release.

Results and discussion

3.1 Introduction of the peptide chemistry N-protection and C-activation

3.1.1 N-Protecting groups

The protection of the α-amino functionality of amino acids is crucial in peptide chemistry to prevent unwanted polymerization once the amino acid is activated. Both in solution-phase and solid-phase peptide synthesis, the α-amino protecting groups need to be removed multiple times during the synthesis. Therefore, the removal should be carried out under mild conditions that do not affect the other protecting groups or the peptide chain.

One of the most widely used protecting groups is tert-butyloxycarbonyl (**Boc**). It provides solubility in common solvents, prevents epimerization during coupling reactions and can be removed quickly and efficiently without generating undesired byproducts. The most common conditions for Boc group removal are 25-50% TFA in CH_2Cl_2. Other acids such as TMS-Cl phenol at 1M in CH_2Cl_2, 4M HCl in dioxane and 2M $MeSO_3H$ in dioxane have also been successfully used. The Boc group is stable towards bases, nucleophiles and catalytic hydrogenation.

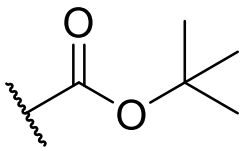

Figure 3.1: *Boc protecting group.*

The reaction of amine protection is carried out using Boc_2O and a base, as shown in *Scheme 3.1*:

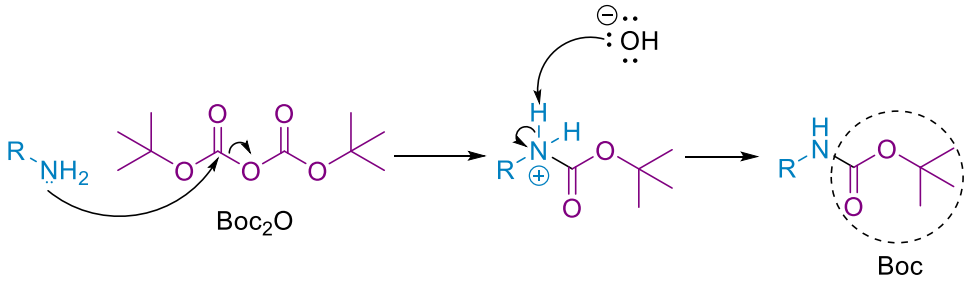

Scheme 3.1: *Mechanism of amine protection with Boc_2O.*

Another widely used protecting group is the benzyloxycarbonyl (**Z or Cbz**) group. It is chosen for its easy preparation of Z-protected amino acids high stability of protected amino acids and peptides, resistance to mild bases and acids and the availability of various removal conditions. The Z group can be removed through catalytic hydrogenation or by using strong acids such as HBr in acetic acid, high-temperature TFA, TFA-thionisole, liquid HF or BBr_3. Additionally, the Z group suppresses racemization during peptide bond formation.[20]

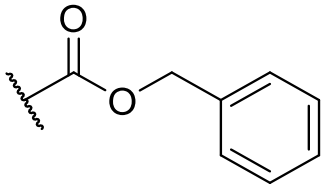

Figure 3.2: *Z (or Cbz) protecting group.*

The reaction mechanism for protecting amines using the Z protecting group is shown in ***Scheme 3.2***:

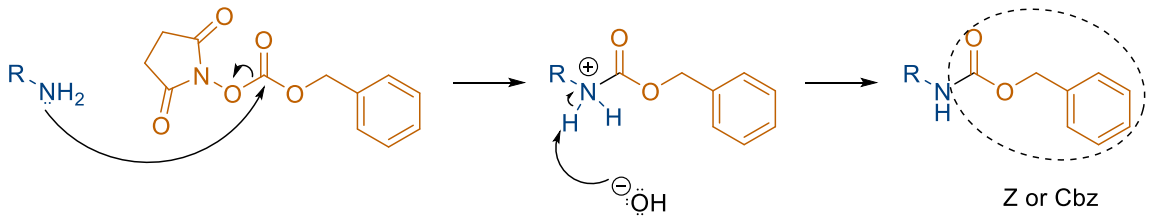

Scheme 3.2: *Mechanism of amine protection with Z (or Cbz).*

[20] Isidro-Llobet, A., Álvarez, M., & Albericio, F. (**2009**). "Amino Acid-Protecting Groups." *Chemical Reviews, 109*(6), 2455-2504.

3.1.2 Amino acid activation

During peptide synthesis, it is necessary to activate amino acids to facilitate the formation of peptide bonds, as the spontaneous reaction between a carboxylic group (-COOH) and an amino group ($-NH_2$) is not favorable due to their low reactivity. By activating the amino acids, their reactivity is increased, allowing the carboxylic group of one amino acid to react with the amino group of another amino acid to form an amide bond. The activation of the carboxylic group involves converting it into a more reactive species, which facilitates the coupling reaction. Some commonly used coupling reagents are carbodiimides[21] and those based on phosphonium or aminium salts (also known as uronium).

The most common carbodiimides are DCC and DIC. Their reaction with carboxylic acid produces a highly reactive O-acylurea, which readily reacts with the amino group of another amino acid to form the peptide bond. However, carbodiimides can be problematic as they are highly reactive and can lead to racemization of the amino acid.

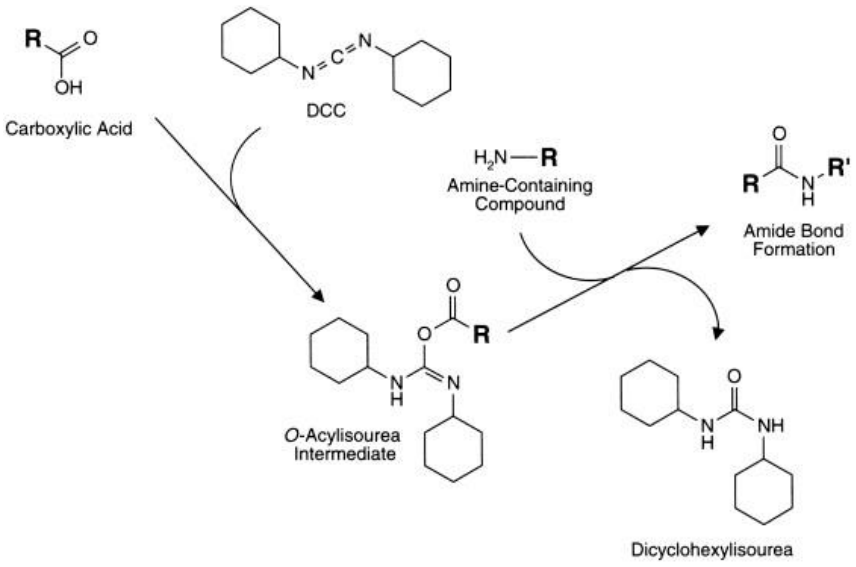

Scheme 3.3: Peptide bond formation through DCC.

[21] Collaborators of Wikipedia. (2021). "Peptide synthesis". Wikipedia, the free encyclopedia.

Coupling agents based on phosphonium or aminium salts, in the presence of a tertiary base, can efficiently convert protected amino acids into various activated species. The reagents BOP, PyBOP and HBTU generate OBt esters, while HATU2, PyAOP1,3 and HCTU4, PyClocK generate OAt y O-6-ClBt esters, respectively. Coupling reagents based on the Oxyma Pure leaving group have also been introduced, which are not potentially explosive as they are not based on triazole reagents.

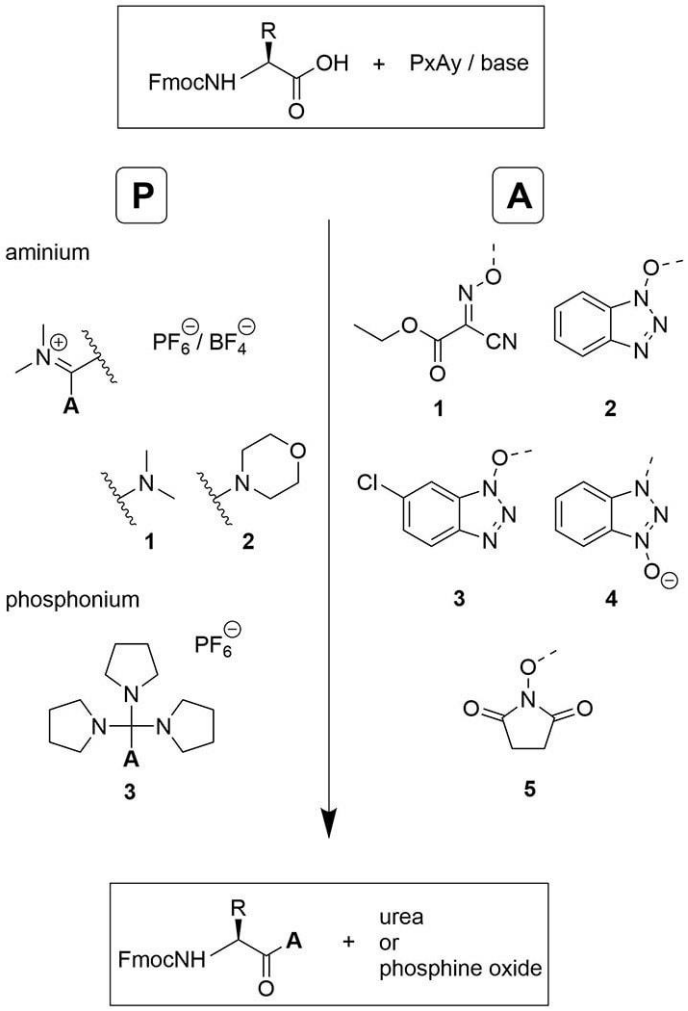

P1A1 = TOTU , P1A2 = HBTU/TBTU , P1A3 = HCTU , P1A4 = HATU , P1A5 = TSTU
P2A1 = COMU
P3A1 = PyOxim , P3A2 = PyBOP , P3A3 = PyClock , P3A4 = PyAOP

Figure 3.3: Active species (esters) generated by the most common coupling reagents.

3.2 Synthesis of bolaamphiphilic derivatives of L-cystine

The synthesis of three cationic bolaamphiphiles (TriMeC$_6$CysOMe, TriMeC$_6$CysHx, MPCysHx) was attempted, however, only one of them was successfully completed.

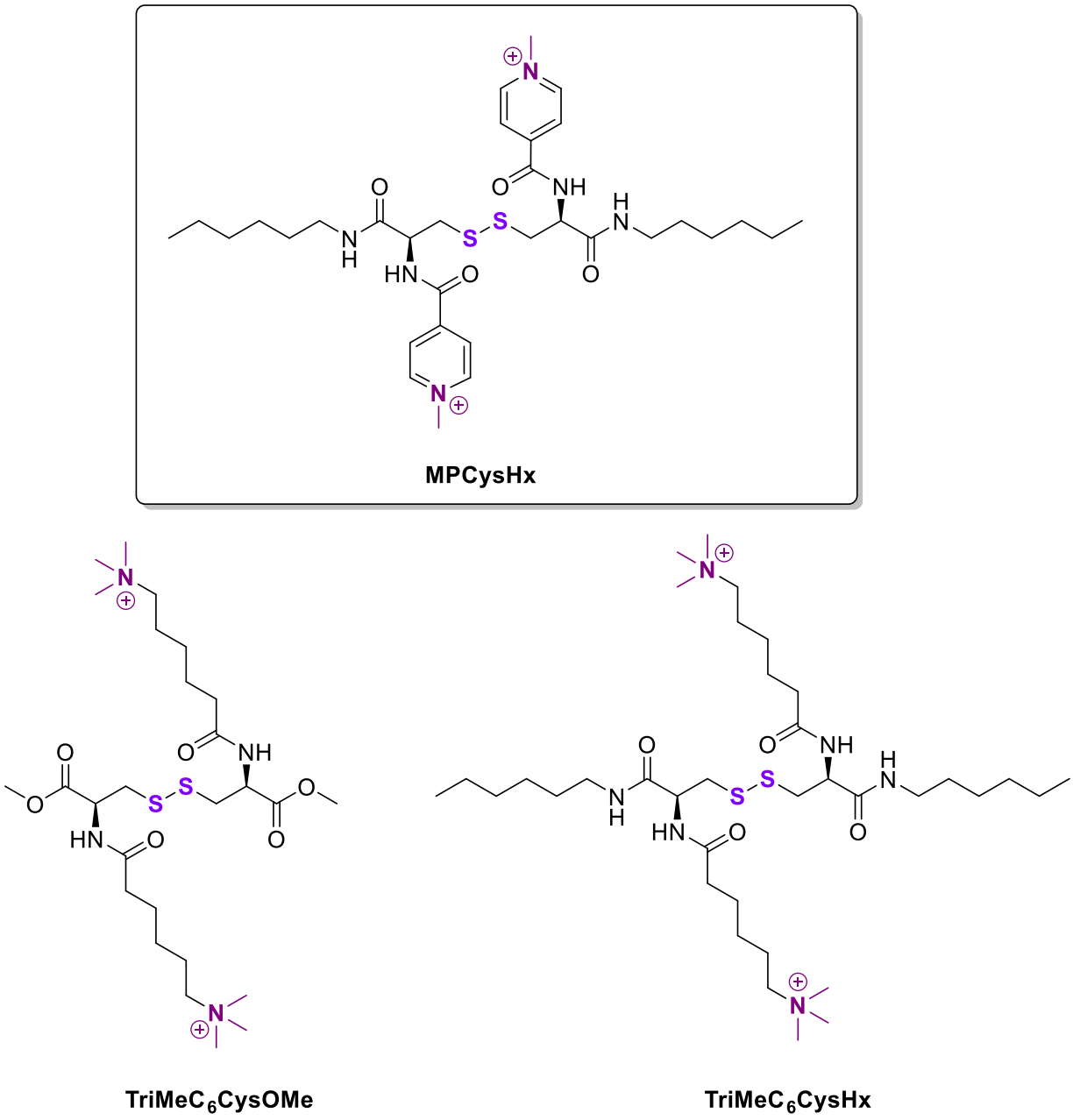

Scheme 3.4: Bolaamphiphilic compounds derived from L-cystine.

3.2.1 Synthetic route 1: Synthesis of MPCysHx

MPCysHx was obtained following the procedure shown in ***Scheme 3.5*** The abbreviation **MPCysHx** originates from **M**ethyl groups attached to the pyridinic nitrogen, **P**yridine-4-carboxylic acid, **Cys**tine and the **Hex**yl alkyl chain. The process is divided into four steps.

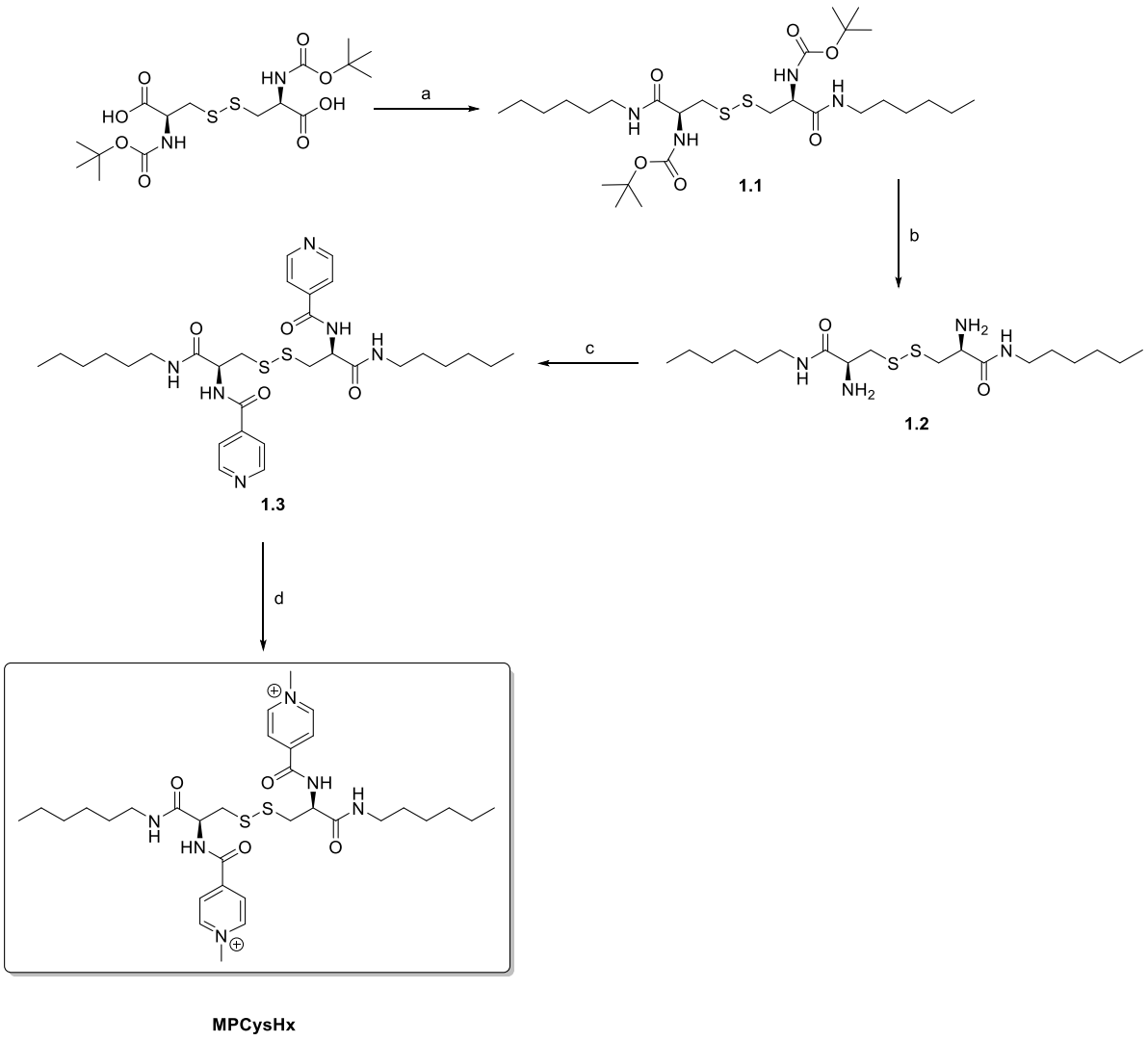

Scheme 3.5. ***Synthetic route 1.*** *Reagents and conditions: a) Hexylamine, TBTU, DIPEA in DMF, rt., overnight, 71% b) TFA in CH_2Cl_2, rt., 2h, then NaOH, 81% c) Pyridine-4-carboxylic acid, TBTU, DIPEA in $CHCl_3$, rt., overnight, 91% d) CH_3I in ACN, 60 °C, overnight, 81%.*

- Step **a**: A coupling reaction is performed between N-protected L-Cystine and hexylamine (both commercially available reagents). The coupling reaction takes place in the presence of the coupling agent TBTU and DIPEA, resulting in the formation of an amide bond between these compounds.
- Step **b**: The Boc protecting group is removing using TFA dissolved in CH_2Cl_2. The aim of this step is to deprotect the amine group of cystine, allowing for another subsequent coupling reaction.
- Step **c**: Another coupling reaction is carried out between the modified cystine compound and pyridine-4-carboxylic acid. The coupling reaction takes place in the presence of TBTU and DIPEA, resulting in the formation of another amide bond.
- Step **d**: The pyridinic nitrogen atoms are methylated using CH_3I. The purpose of this step is to introduce positive charges on the pyridinic nitrogen atoms, resulting in the formation of the final cationic compound.

The mechanism of the TBTU coupling agent for forming peptide bonds (steps **a** and **c** of *synthetic route 1*) is depicted in ***Scheme 3.6***:

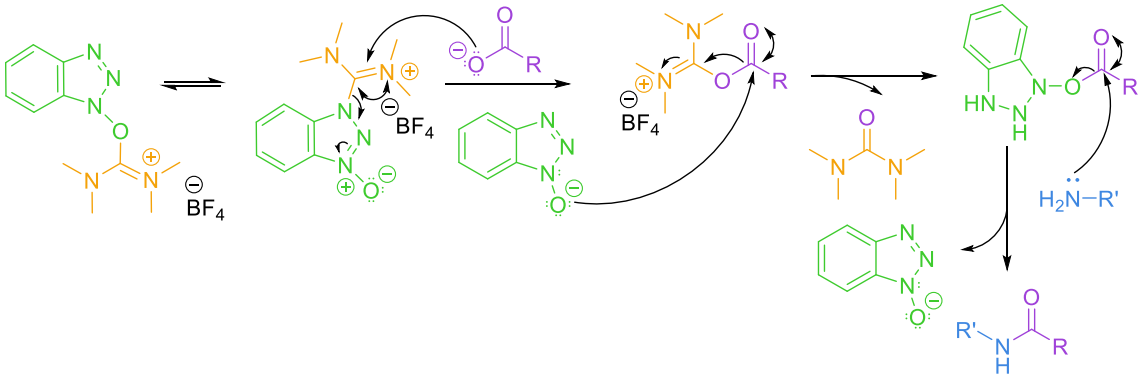

Scheme 3.6: *Reaction mechanism of the coupling between carboxylic acids and primary amines promoted by TBTU.*

The mechanism of the amine deprotection reaction using TFA (step **b** of *synthetic route 1*) is depicted in ***Scheme 3.7***:

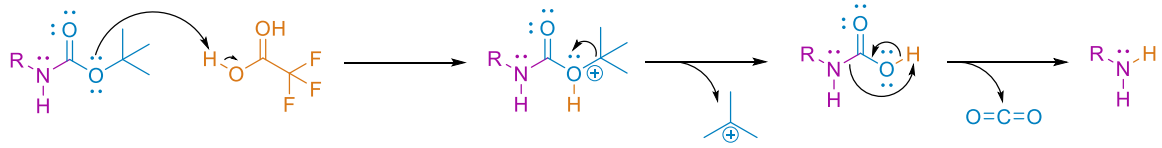

Scheme 3.7: *Reaction mechanism for amine deprotection using TFA.*

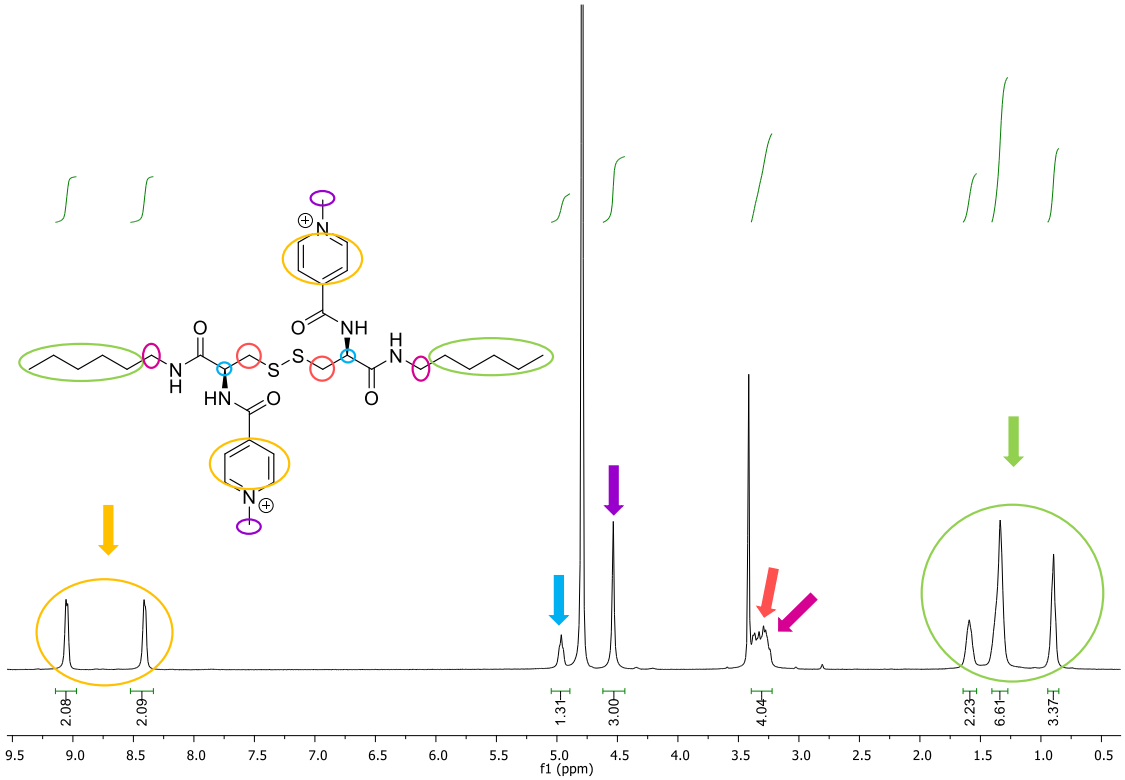

Figure 3.4: *^{1}H-NMR spectra of MPCysHx at 400 MHz in D_2O.*

The ^{1}H-RMN spectra of the final cationic compound MPCysHx (***Figure 3.4***) reveals two doublets between 9.1 and 8.4 ppm corresponding to the protons of the pyridines. Around 5 ppm, the signal referring to the proton of the chiral carbon appears and slightly above 4.5 ppm, the signal corresponding to the protons of the methyl group attached to the pyridinic nitrogen is observed (this signal confirms the successful methylation). Below 3.4 ppm, the signals of the diastereotopic protons of the methylene adjacent to sulfur and the methylene of the aliphatic chain closest to the amide bond overlap. Finally, between 1.6 and 0.9 ppm, the signals corresponding to the protons of the aliphatic chain are observed.

It is important to note that due to the deuterated solvent used to obtain the spectra (D_2O in this case), the protons of the amides are not observed because they undergo very fast exchange with it.

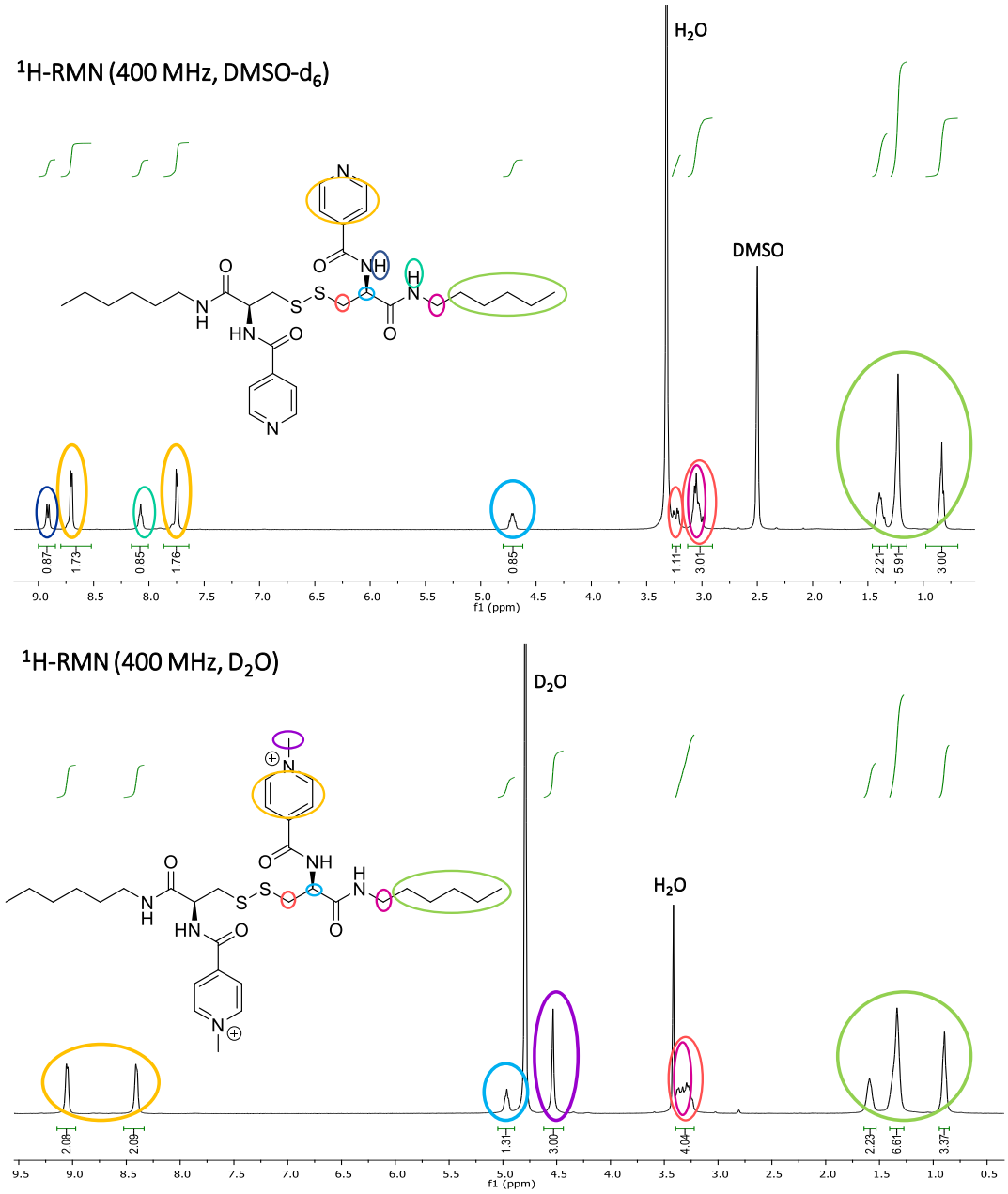

Figure 3.5: *Comparison between the 1H-RMN spectra of compound 1.3 (up) and MPCysHx (down).*

3.2.2 Synthetic route 2: Synthesis of TriMeC$_6$CysOMe

TriMeC$_6$CysOMe was obtained following the procedure shown in ***Scheme 3.8***. The abbreviation **TriMeC$_6$CysOMe** comes from the terminal **TriMe**thylated amine followed by a 6-carbon aliphatic chain (**C$_6$**), the central **Cys**tine and the **O-Me**thylated carboxylic acid. The process is divided in five steps:

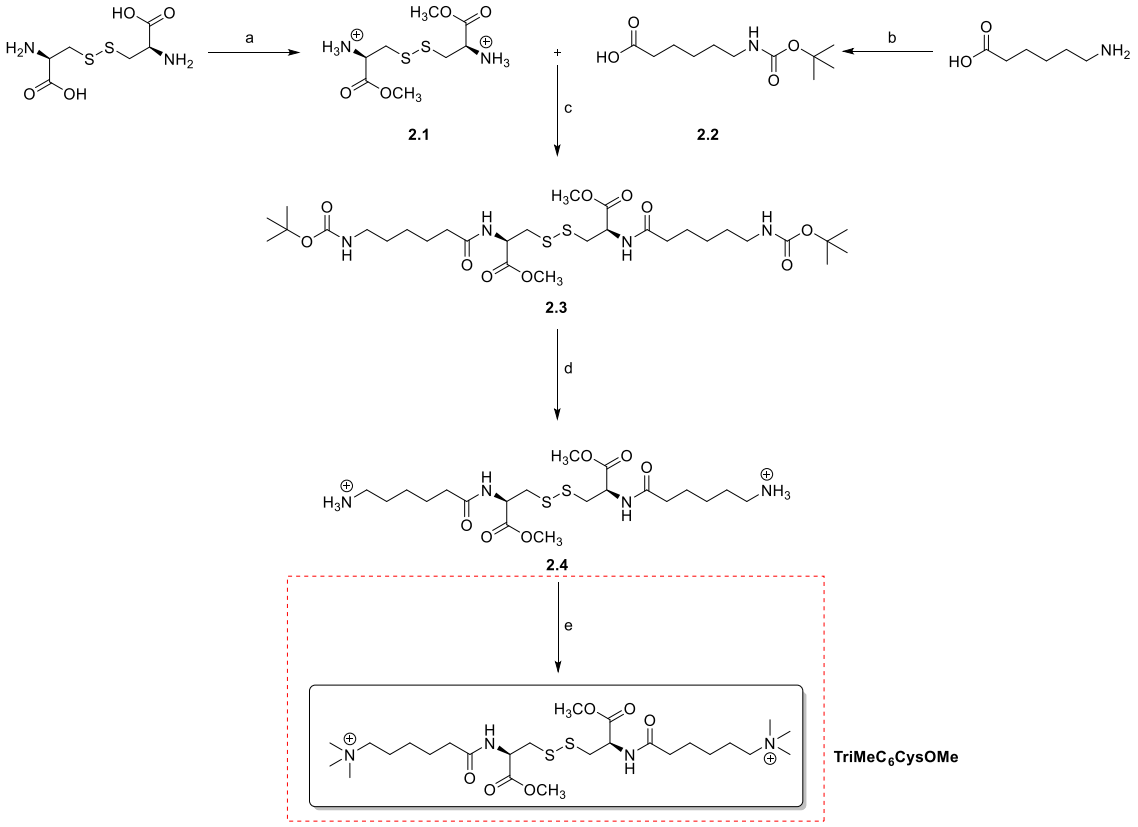

Scheme 3.8. *Synthetic route 2. Reagents and conditions of: a) L-Cystine, $SOCl_2$ in MeOH, 70°C, 21h, 99% b) 6-aminohexanoic acid, Boc_2O in Dioxane/H_2O, rt., 2h, 82% c) 6-((tert-butoxycarbonyl)amino)hexanoic acid, TBTU, DIPEA in CH_2Cl_2, rt., overnight, 91% d) TFA in CH_2Cl_2, rt., 2h, 95% e) CH_3I in ACN, K_2CO_3, rt., overnight, 11%.*

- Step **a**: Firstly, the carboxylic acid of L-cystine is activated by converting it into an acid chloride using $SOCl_2$. Subsequently, it reacts with MeOH, resulting in methylation (actually esterification). This allows for the subsequent coupling to occur through the amine.
- Step **b**: The amine of 6-aminohexanoic acid is protected using the Boc protecting group, so that the coupling can later occur through the carboxylic acid position.
- Step **c**: A coupling reaction takes place between the derived molecule of L-cistine through the amine position and the N-protected 6-aminohexanoic acid, in the presence of the coupling agent TBTU and DIPEA.
- Step **d**: Deprotection of the Boc protecting group is carried out using TFA dissolved in CH_2Cl_2, aiming to free the amine and enable its trimethylation to obtain the final cationic compound.

  After performing step **e** (which involved trimethylation in the presence of K_2CO_3 and CH_3I), when characterizing the obtained compound using ^{1}H-NMR, the expected signals were not observed. Instead, what was observed was the disappearance of the signals corresponding to the protons neighboring the disulfide bond.

Since the final product could not be obtained, there is no ^{1}H-NMR spectra available for the final product TriMeC_6CysOMe.

3.2.3 Synthetic route 3: Synthesis of TriMeC$_6$CysHx

TriMeC$_6$CysHx was obtained following the procedure shown in ***Scheme 3.9***. The abbreviation **TriMeC$_6$CysHx** comes from the terminal **TriMe**thylated amine followed by a 6-carbon aliphatic chain (**C$_6$**), the central **Cys**tine and the **Hex**yl alkyl chain. The process is divided in five steps:

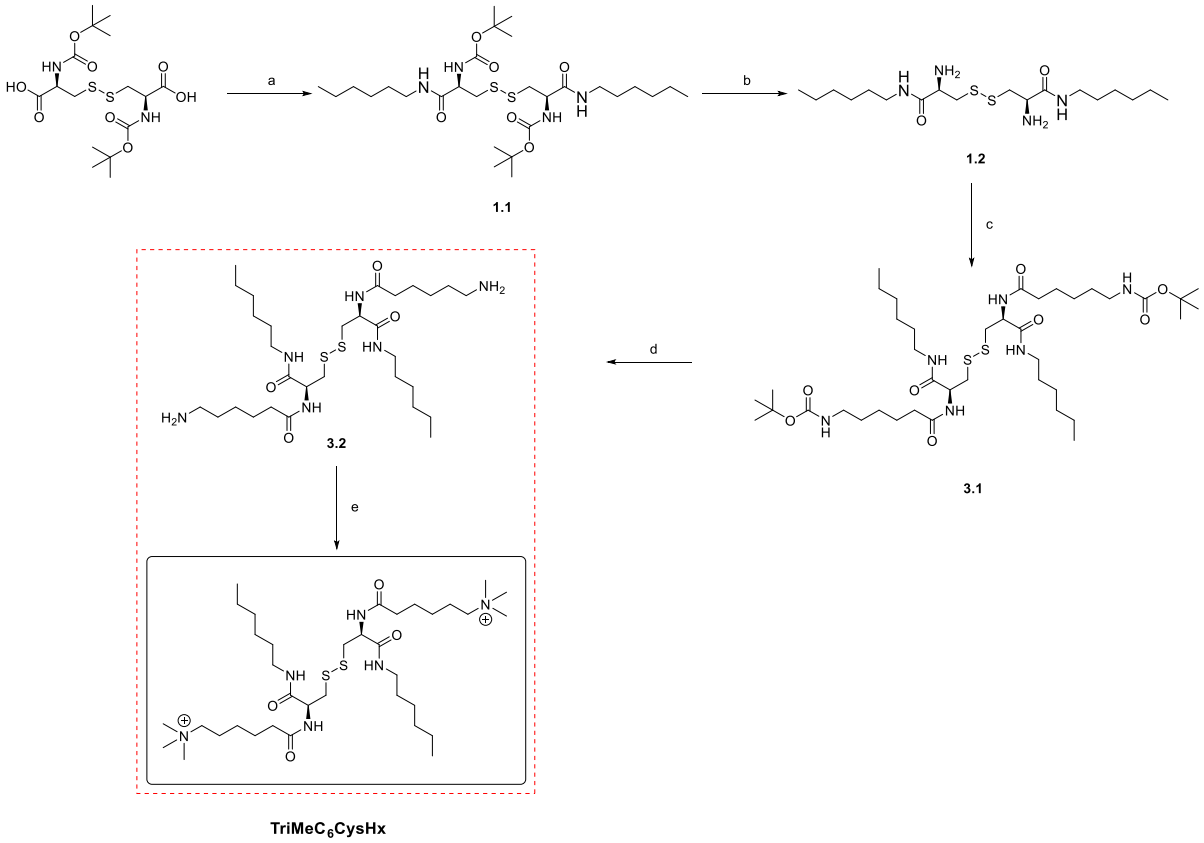

Scheme 3.9. *Synthetic route 3. Reagents and conditions of: a) Hexylamine, TBTU, DIPEA in DMF, rt., 16h, 71% b) TFA in CH_2Cl_2, rt., 2h, then NaOH, 81% c) 6-((tert-butoxycarbonyl)amino)hexanoic acid, TBTU, DIPEA in CH_2Cl_2, rt., overnight, 57% d) TFA in CH_2Cl_2, NaOH, rt., 2h e) It was not carried out.*

The first two steps, **a** and **b**, are identical to those carried out in ***synthetic route 1***, resulting in the same intermediates. These steps are described in section **3.2.1**.

In the step **c**, a coupling reaction occurs between 6-((tert-butoxycarbonyl)amino)hexanoic acid (compound **2.2,** an intermediate of *synthetic route 2*) and compound **1.2** (an intermediate of *synthetic route 1*) in the presence of TBTU and DIPEA.

After performing step **e** (which involved the removal of the Boc protecting group that protected the terminal amines suing TFA dissolved in CH_2Cl_2, followed by basification with NaOH to convert the ammonium salt into free amine), upon characterizing the obtained product using ^{1}H-NMR, the signals corresponding to the expected product were not observed. Additionally, there was a color variation of the compound (from white to brown) and a distinct sulfur odor was perceived. After this occurrence, step **e** was not carried out.

Since the final product could not be obtained, there is no ^{1}H-NMR spectra vailable for the final product TriMeC_6CysHx.

3.3 Aggregation studies

3.3.1 UV-Vis and fluorescence spectroscopy studies

After synthesizing the final cationic compound, MPCysHx, a proof-of-concept test was conducted to determine if the compound could aggregate in an aqueous medium and have the ability to encapsulate molecules. For this purpose, Nile Red, a lipophilic dye that has an affinity for lipids and can easily penetrate cell membranes and lipid structures, was used.

Nile Red is not strongly fluorescent in most polar solvents, such as water. However, when it is in a lipophilic or nonpolar environment, such as the interior of the synthesized bolaamphiphilic structure, it becomes intensely fluorescent.

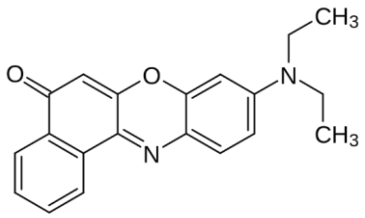

Figure 3.6: Chemical structure of Nile Red.

Figure 3.7 shows the test that confirms that the synthesized compound is indeed capable of aggregation in aqueous media and trapping lipophilic compounds like Nile Red.

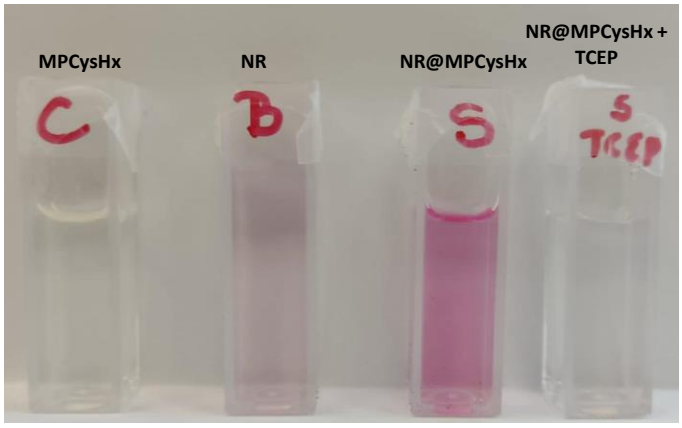

Figure 3.7: Picture of the cuvettes used in the evaluation of the incorporation of Nile Red (NR) into MPCysHx vesicles. TCEP is the reducing agent that provokes disulfide reduction. [MPCysHx] = 5 mM; [NR] = 10 μM.

In *Figure 3.7*, the left cuvette labeled as C contains only the synthesized compound MPCysHx with a concentration of 5 mM dissolved in distilled water. As observed, it is colorless. The next cuvette, labeled as B, contains only the Nile Red dye with a concentration of 10 µM dissolved in water, exhibiting weak fluorescence. The cuvette labeled as S contains the synthesized compound MPCysHx along with the Nile Red dye in water. In this case, a significant increase in the color of the solution is observed, confirming that our bolaamphiphilic compound aggregates in an aqueous medium and can encapsulate the lipophilic dye. Finally, in the right cuvette labeled as S TCEP, the Nile Red dye, the synthesized compound and the reducing agent TCEP are present. This last test was conducted to verify if our bolaamphiphilic compound, having a disulfide bond, is sensitive to reducing environments. The disappearance of coloration in the solution confirms that the bolaamphiphilic compound, in the presence of reducing agents, breaks apart and releases the cargo stored inside.

The absorbance and fluorescence spectra of the previous samples are shown in the following figures.

Figure 3.8, shows that in the presence of MPCysHx a absorption band corresponding to Nile Red is observable with a maximum at 525 nm. Addition of the reducing agent TCEP provokes a dramatic decrease of the absorbance, indicating vesicle disassembly and release of Nile Red to the aqueous environment.

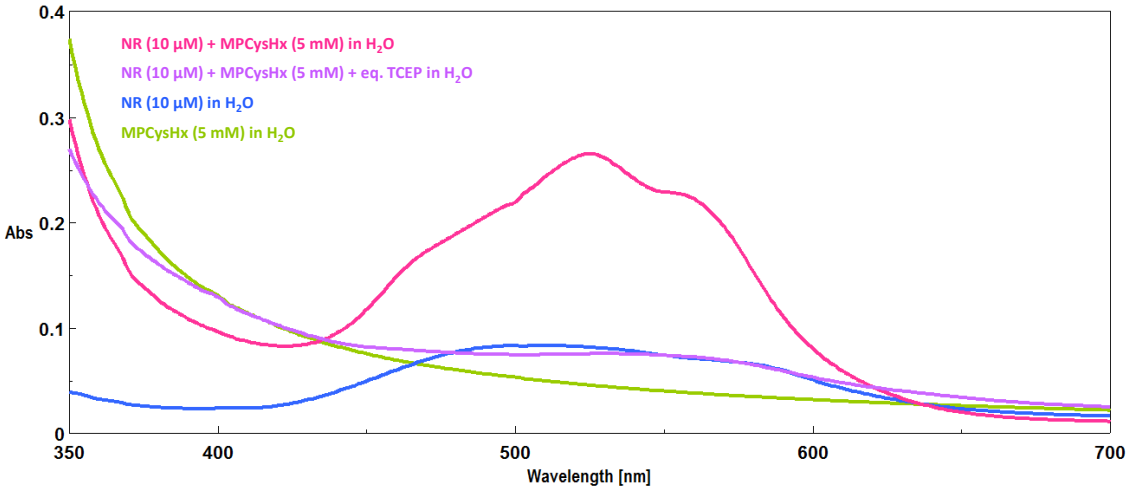

Figure 3.8: *UV-Vis absorbance spectra corresponding to the study of loading and release of Nile red into MPCysHx vesicles (25 ºC).*

In the case of the fluorescence spectra (***Figure 3.9***), a dramatic increase in fluorescent emission was observed upon loading of Nile Red into MPCysHx vesicles, with a maximum at 580 nm. Again, addition of TCEP causes a fluorescence quenching as result of the release of Nile to the medium.

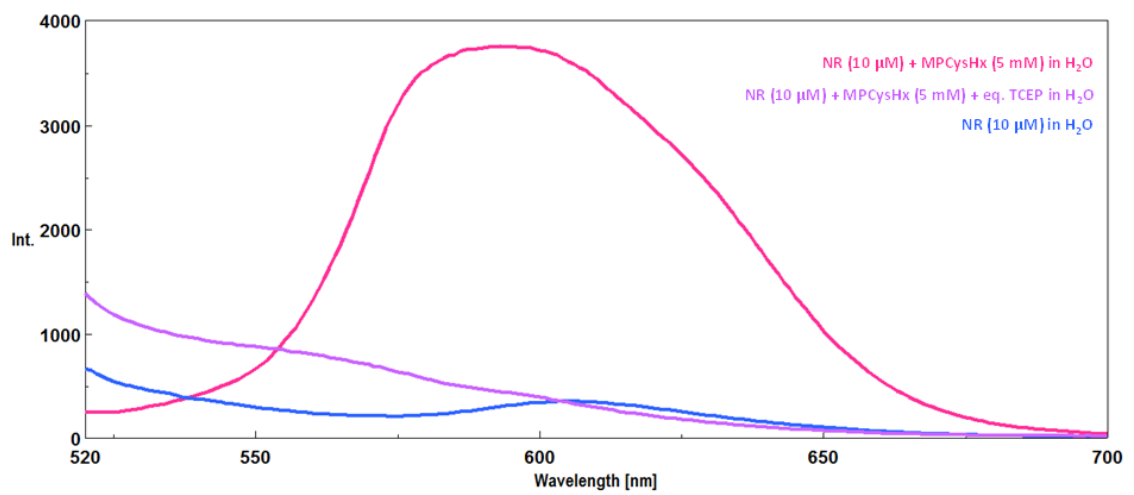

Figure 3.9: *Fluorescence spectra corresponding to the study of loading and release of Nile red into MPCysHx vesicles (λ_{exc} = 500 nm; 25 ºC).*

3.3.2 Dynamic Light Scattering (DLS) studies

DLS analysis was performed to determine the size of the formed vesicles. This technique analyses the light scattering of the sample to obtain the particle diffusion rate. From that, using the Stokes-Einstein equation, a diameter can be calculated considering spherical particles.

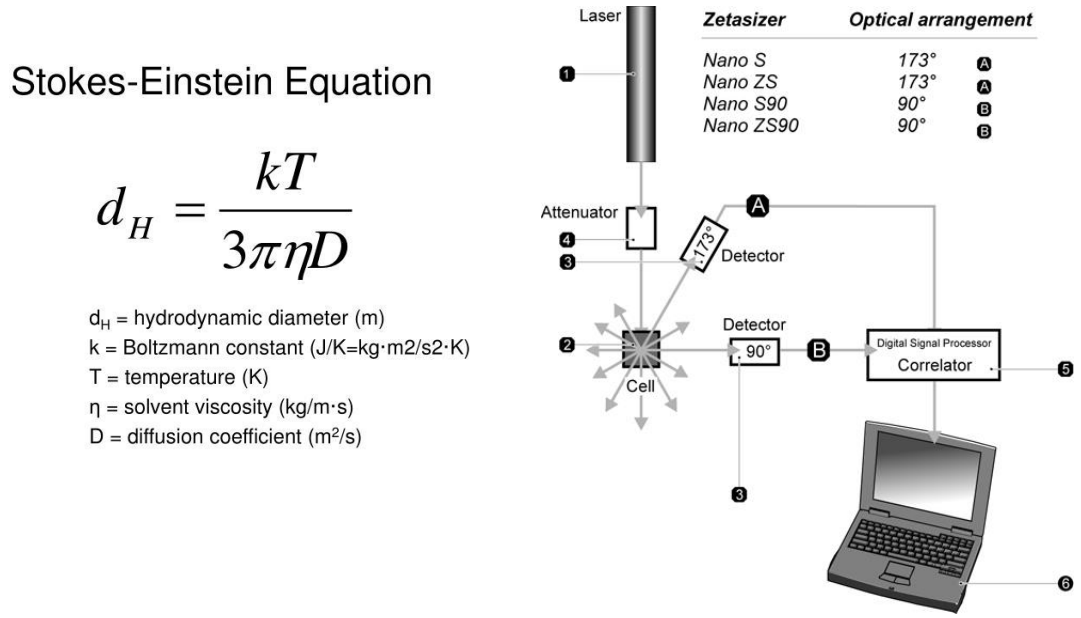

Figure 3.10. Stokes-Einstein equation and scheme of a DLS device.

Figure 3.10, shows the diameter distribution obtained for a 5 mM sample of MPCysHx in water. A monomodal distribution is obtained with an average diameter of 133 ± 57 nm. The size dispersion is measured with the so-called polydispersity index, PdI, which by analyzing the autocorrelation function obrtained in the DLS measurement. PdI range from 1 (infinitely dipersed samples) to 0 (perfectly monodisperse sample). In this case a value of 0.27 was obtained, which indicates a moderate polydispersion.

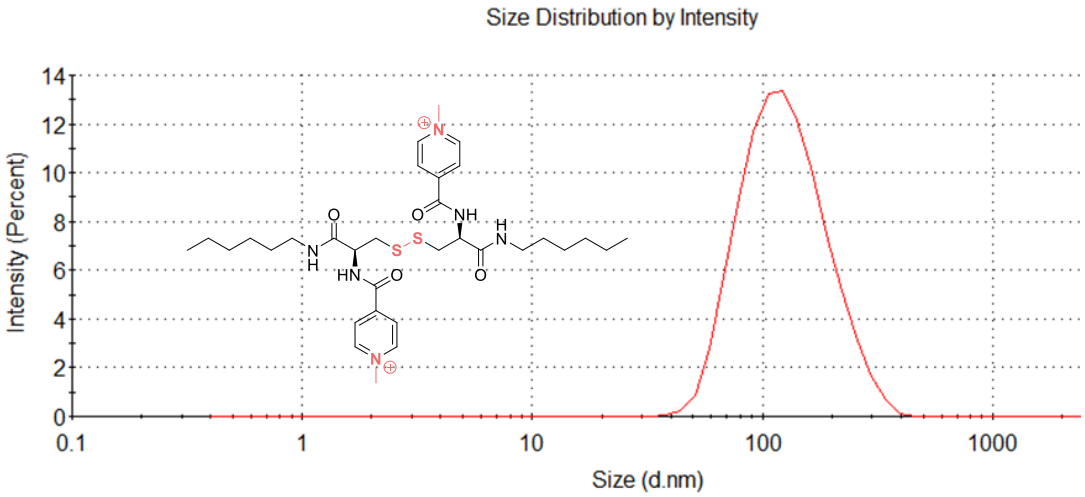

Figure 3.10: *Size distribution of the vesicles obtained by DLS in water for a 5 mM sample of MPCysHx. (25 ºC).*

3.3.3 Determination of the critical aggregation concentration (CAC) of MPCysHx

To evaluate the range of concentrations where vesicles of MPCysHx are formed, the critical aggregation concentration value was determined. For this purpose, the light dispersed at 700 nm was measured in the UV-Vis spectrometer. The formation of particles results in light dispersion which results in an increase in the observed absorbance values. In ***Figure 3.11***, can be seen that the aborbance is almost unvariable when the concentration of MPCysHx is the range 0 – 1 mM. At 2 mM a discontinuity is observed with a notable absobance increase, pointing to the formation of vesicles. From 2 to 8 mM the absorbance shows a plateau but a further discontinuity arises at 9 mM. This could be the result of vesicle aggregation or their restructuration to larger diameters.

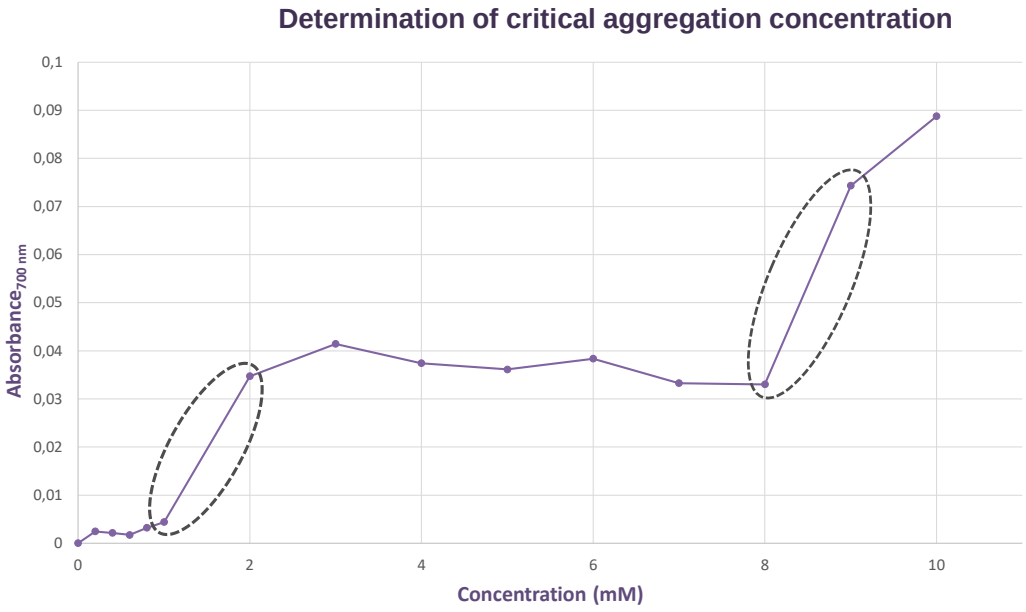

Figure 3.11: *Variation of the aborbance at 700 nm with the concentration of MPCysHx in water at 25 ºC.*

Conclusions

- ✓ The cationic bolaamphiphilic compound **MPCysHx** is capable of forming aggregates in an aqueous medium. Specifically, at a concentration of 2 mM, the compound is capable of forming vesicles, and at 9 mM, there is the possibility of vesicle aggregation or restructuring into larger diameter vesicles.

- ✓ For a 5 mM sample of **MPCysHx** in water, DLS studies yield an average diameter of 133 ± 57 nm.

- ✓ **MPCysHx** is capable of encapsulating hydrophobic dyes such as Nile Red within its interior and it is sensitive to reducing agents like TCEP.

- ✓ The synthetic routes for obtaining the compounds **TriMeC$_6$CysOMe** and **TriMeC$_6$CysHx** did not work as expected, and therefore, they could not be obtained.

Based on the results obtained, it can be concluded that the cationic bolaamphiphilic compound derived from L-cystine, **MPCysHx**, could be promising for use as a nanocarrier for anticancer drugs with low solubility in water, offering new perspectives in the field of cancer therapy.

Experimental section

5.1 General methods

$^{1}H/^{13}C$ NMR spectra were recorded at 400/101 MHz or 300/75 MHz in the indicated solvent at 30°C. Signals of the deuterated solvent were taken as the reference in DMSO-d_6, the singlet at δ 2.50 and the quadruplet centered at 39.52 ppm, in $CDCl_3$, the singlet at δ 7.26 and the singlet at 77.16 ppm and in D_2O the singlet at δ 4.79 ppm for ^{1}H and ^{13}C NMR, respectively.

Mass spectra were recorded with a mass spectrometry triple quadrupole Q-TOF Premier spectrometer (Waters) with simultaneous Electrospray and APCI Probe.

The absorbance and fluorescence properties were measured with a JASCO V-630 UV-Vis spectrophotometer and a JASCO FP-8300 fluoremeter, both equipped with a Peltier accessory measured at 25°C.

Light Scattering (DLS) measurements were recorded using a Zetasizer Nano ZS (Malvern Instruments, UK), using 3 mL disposable poly(methylmethacrylate) cuvettes (10 mm optical path length). Analyses were carried out using a He-Ne laser (633 nm) at a fixed scattering angle of 173°. Automatic optimization of beam focusing and attenuation was applied for each sample. The results were reported as the average of three measurements.

Reactions that required an inert atmosphere were carried out under N_2.Comercially available reagents were used as received, without further purification.

5.2 Experimental procedure

5.2.1 Experimental procedure for the synthesis of MPCysHx

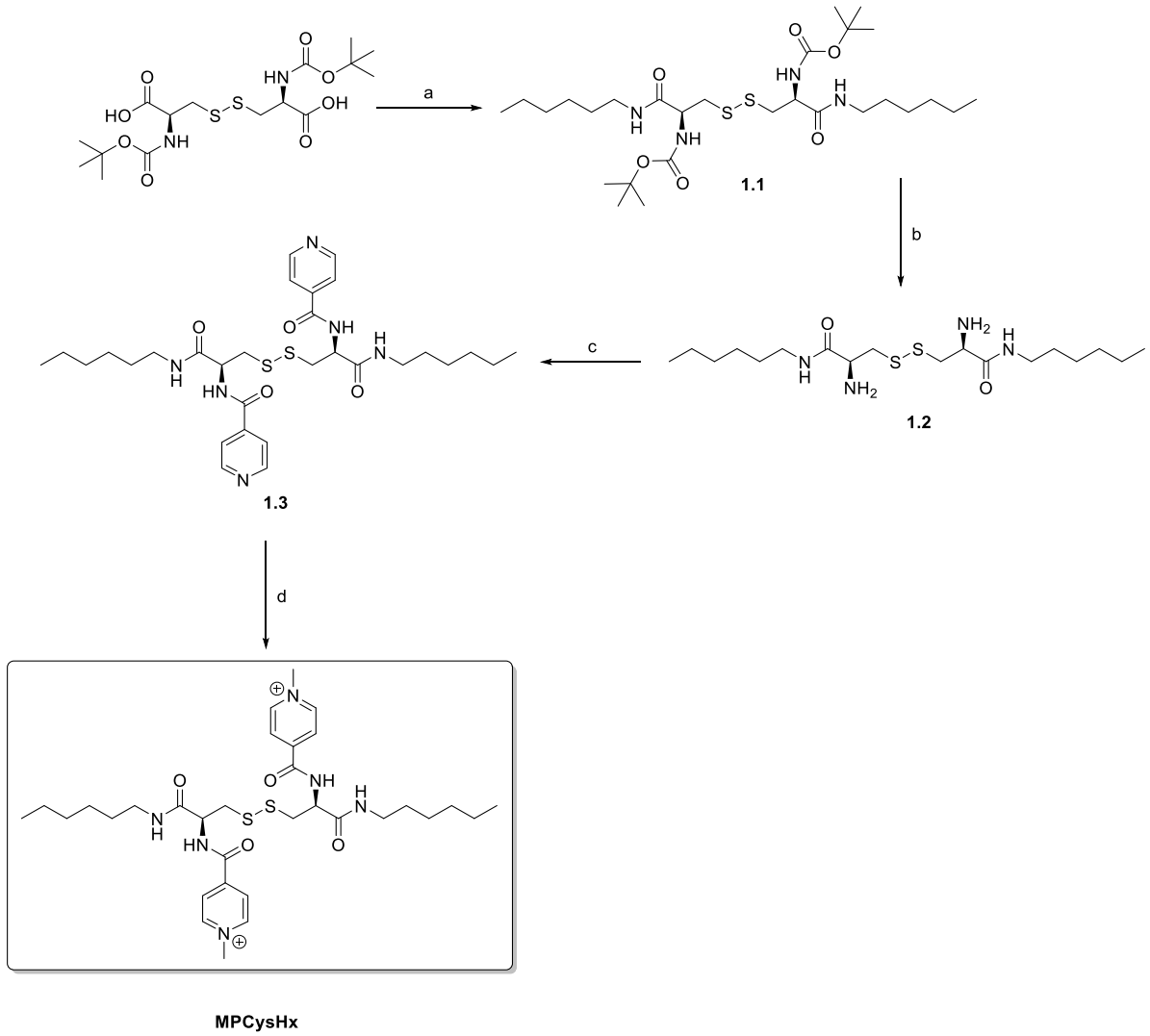

Scheme 5.1. Synthetic route 1. Reagents and conditions: a) Hexylamine, TBTU, DIPEA in DMF, rt.,overnight, 71% b) TFA in CH_2Cl_2, rt., 3h, then NaOH, 81% c) Acid nicotinic, TBTU, DIPEA in $CHCl_3$, rt., overnight, 91% d) CH_3I in ACN, 60°C, overnight, 81%.

5.2.1.1 Coupling between N-protected L-cystine and hexylamine

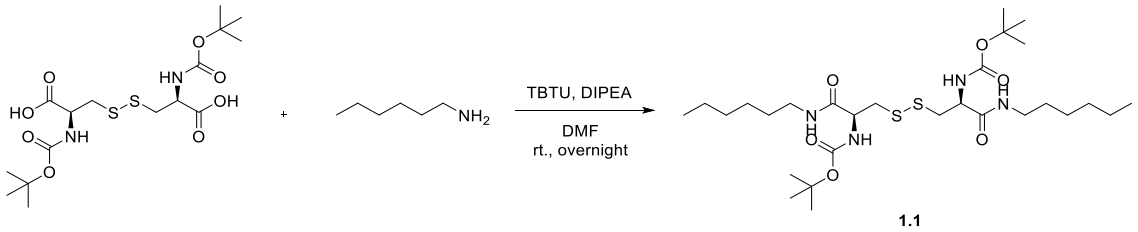

1.1

To a solution of N-protected L-cystine (9.3 mmol, 1eq.) in DMF (150 mL) under N_2 atmosphere and at room temperature, sequentially TBTU (18.8 mmol, 2.02 eq.), hexylamine (18.8 mmol, 2.02 eq.) and DIPEA (18.8 mmol, 2.02 eq.) were added. The resulting mixture was stirred overnight. After this time, distilled water was added to the solution until the formation of a white precipitate was observed. The precipitate was filtered and washed with acidic water, basic water and finally with distilled water to remove residual reagents and reaction by-products. The solid was vacuum-dried overnight at 50°C.

Compound 1.1: Di-tert-butyl((2S, 2'S)-disulfanediiylbis(3-(hexylamino)-3-oxopropane-1,2-diyl))dicarbamate

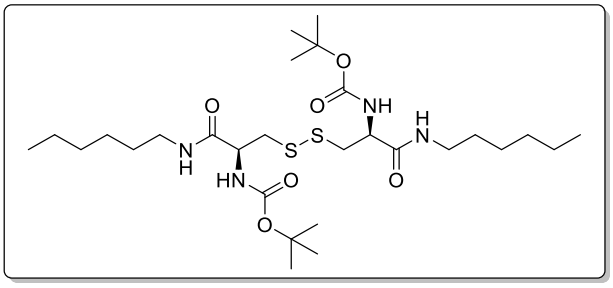

Yield: 71 % (4.0 g, 6.59 mmol)

^{1}H-NMR (400 MHz, DMSO-d$_6$): δ 7.83 (s, 1H), 6.95 (d, *J* = 8.3 Hz, 1H), 4.13 (m, 1H), 3.13-2.96 (m, 3H), 2.90-2.73 (m, 1H), 1.38 (m, 11H), 1.24 (m, 6H), 0.85 (t, *J* = 6.5 Hz, 3H).

^{13}C-NMR (101 MHz, DMSO-d$_6$): δ 169.94 (C=O), 155.16 (C=O), 78.27 (C), 53.67 (CH), 40.46 (CH_2), overlapping with signals of the deuterated solvent, 30.94 (CH_2), 28.88 (CH_2), 28.11 (CH_3), 25.89 (CH_2), 22.00 (CH_2), 13.86 (CH_3).

HRMS (ESI-TOF) m/z: $[M+Na]^+$ Calcd for $C_{28}H_{54}N_4O_6S_2$: 606,882; Found: 629.3382

5.2.1.2 Removal of the Boc protecting group with TFA

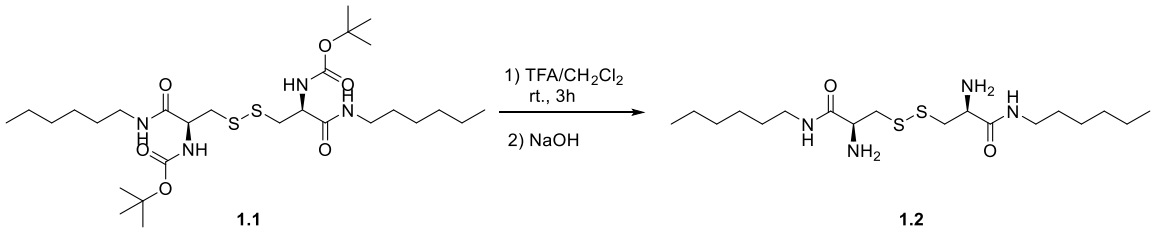

To a solution of compound **1.1** (6.59 mmol, 1eq.) in CH_2Cl_2 (150 mL), TFA (287.29 mmol, 43.6 eq.) dissolved in CH_2Cl_2 (50 mL) was added under N_2 atmosphere at room temperature. The resulting mixture was stirred for 3h. After this time, the solution was concentrated under vacuum until dryness. Then, it was dissolved in distilled water (300 mL) and solid NaOH was slowly added until reaching a pH of 10-11. The mixture was extracted three times with chloroform. The combined organic layers were then dried over anhydrous MgSO4, filtered and concentrated to dryness under reduced pressure.

Compound 1.2: (2S, 2'S)-3,3-disulfanediylbis(2-amino-N-hexylpropanamide)

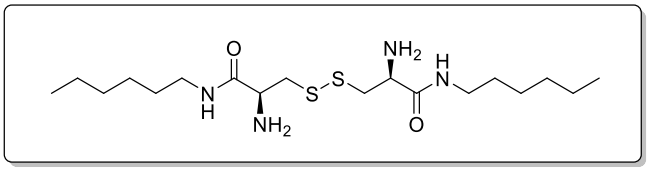

Yield: 81% (2.16 g, 5.31 mmol)

^{1}H-NMR (300 MHz, DMSO-d_6): δ 7.93 (t, *J* = 5.5 Hz, 1H), 3.47-3.34 (m, 1H), 3.05 (tdd, *J* = 13.0, 11.2, 5.9 Hz, 3H), 2.76 (dd, *J* = 13.0, 7.8 Hz, 1H), 1.89 (s, 2H), 1.53-1.14 (m, 8H), 0.86 (t, *J* = 6.6 Hz, 3H).

^{13}C-NMR (75 MHz, DMSO-d_6): δ 172.91 (C=O), 54.22 (CH), 44.56 (CH_2), 38.69 (CH_2), 30.98 (CH_2), 29.02 (CH_2), 26.03 (CH_2), 22.04 (CH_2), 13.90 (CH_3).

HRMS (ESI-TOF) m/z: $[M+H]^+$ Calcd for $C_{18}H_{38}N_4O_2S_2$: 406.648; Found: 407.2514

5.2.1.3 Coupling between compound 1.2 and pyridine-4-carboxylic acid

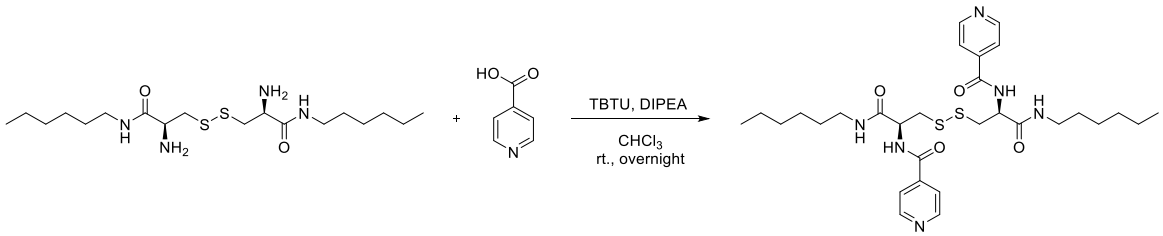

To a solution of compound **1.2** (2.61 mmol, 1 eq.) dissolved in $CHCl_3$ (100 mL) under inert atmosphere of N_2 at room temperature, TBTU (5.27 mmol, 2.02 eq.), pyridine-4-carboxylic acid (5.27 mmol, 2.02 eq.) and DIPEA (5.27 mmol, 2.02 eq.) were sequentially added. The resulting mixture was stirred overnight. After this time, distilled H_2O was added to the solution until the formation of a precipitate was observed. The precipitate was filtered and washed with acidic water, basic water and finally with distilled water. The solid was vacuum-dried overnight at 50°C.

Compound 1.3: N,N'-((2S,2'S)-disulfanediylbis(3-(hexylamino)-3-oxopropane-1,2-diyl))diisonicotinamide

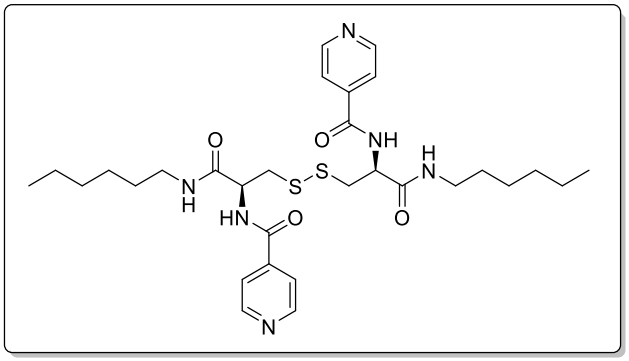

Yield: 91% (1.47 g, 2.38 mmol)

^{1}H-NMR (400 MHz, DMSO-d_6): δ 8.91 (d, *J* = 8.1 Hz, 1H), 8.70 (d, *J* = 5.3 Hz, 2H), 8.07 (s, 1H), 7.76 (t, *J* = 9.5 Hz, 2H), 4.71 (dd, *J* = 13.1, 8.7 Hz, 1H), 3.24 (dd, *J* = 13.5, 4.7 Hz, 1H), 3.13-2.90 (m, 3H), 1.46-1.33 (m, 2H), 1.23 (s, 6H), 0.82 (d, *J* = 6.5 Hz, 3H).

^{13}C-NMR (101 MHz, DMSO-d_6): δ 169.23 (C=O), 164.88 (C=O), 150.08 (CH aromático), 140.80 (C), 121.43 (CH aromático), 52.7 (CH), 39.94 (CH_2), 38.77 (CH_2), 30.90 (CH_2), 28.85 (CH_2), 25.91 (CH_2), 21.98 (CH_2), 13.83 (CH_3).

5.2.1.4 Methylation of the pyridinic nitrogen

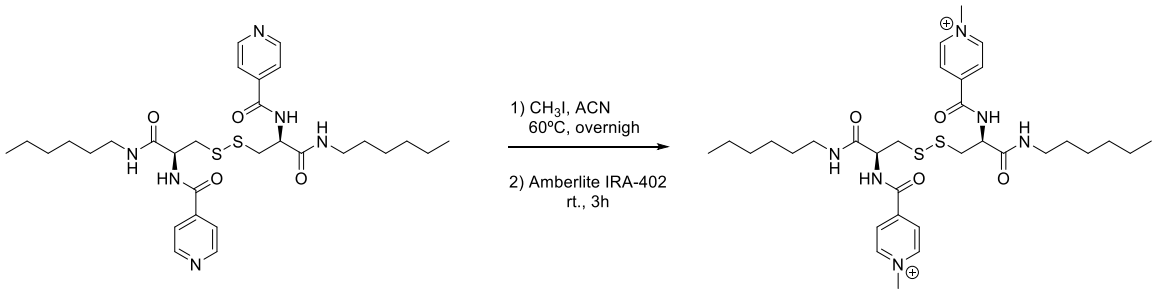

1.3 MPC$_6$CysHx

To a solution of compound **1.3** (2.38 mmol, 1 eq.) in ACN (50 mL), dropwise addition of CH_3I (11.47 mmol, 4.8 eq.) was performed. The resulting mixture was stirred overnight at 60 °C under an inert N_2 atmosphere. After this time, the solution was concentrated under vacuum until dryness. A shiny yellow solid was obtained. Finally, to exchange the iodides for chlorides, the product was dissolved in MeOH and Amberlite IRA-402 (1.9 g) was added and the mix was stirred 3 hours at room temperature. The organic mix was filtered and concentrated to dryness under reduced pressure. This gave final product as an orange solid.

Compound MPC$_6$CysHx: 4,4'-((((2S,2'S)-disulfanediylbis(3-(hexylamino)-3-oxopropane-1,2-diyl))bis(azanediyl)bis(carbonyl))bis(1-methylpyridin-1-ium)

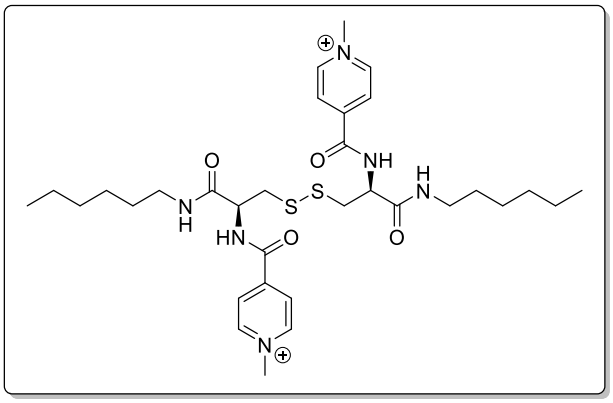

Yield: 98% (2.1 g, 2.33 mmol)

^{1}H-NMR (400 MHz, D_2O): δ 9.05 (d, *J* = 5.2 Hz, 2H), 8.41 (s, 2H), 4.96 (s, 1H), 4.53 (s, 3H), 3.32 (dd, *J* = 25.6, 10.8 Hz, 4H), 1.59 (s, 6H), 0.90 (s, 3H).

^{13}C-NMR (101 MHz, D_2O): δ 170.77 (C=O), 164.83 (C=O), 147.89 (C), 146.43 (CH), 126.13 (CH), 54.05 (CH), 48.94 (CH_3), 39.70 (CH_2), 38.58 (CH_2), 30.68 (CH_2), 28.17 (CH_2), 25,71 (CH_2), 21.96 (CH_2), 13.35 (CH_3).

5.2.2 Experimental procedure for the synthesis of TriMeC$_6$CysOMe

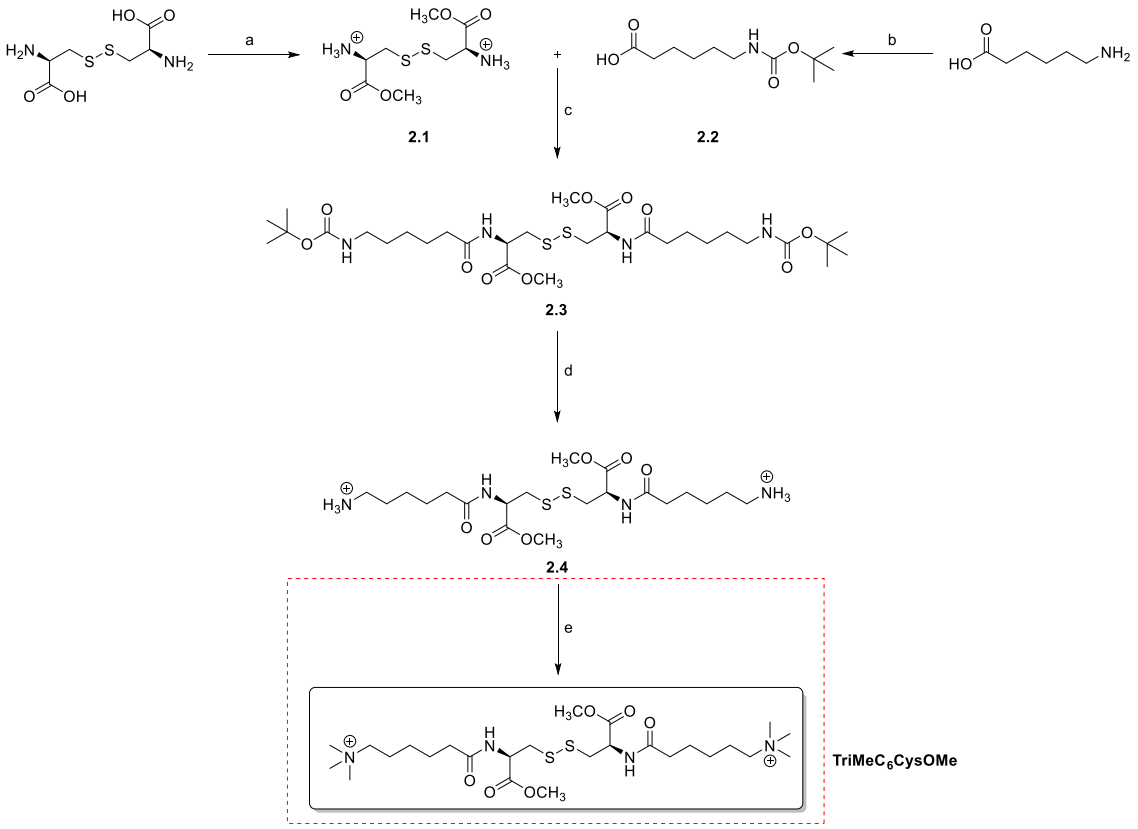

Scheme 5.2. Synthetic route 2. Reagents and conditions: a) L-Cystine, $SOCl_2$ in MeOH, 70°C, 21h, 99% b) 6-aminohexanoic acid, Boc_2O in Dioxane/H_2O, rt., 2h, 82% c) 6-((tert-butoxycarbonyl)amino)hexanoic acid, TBTU, DIPEA in CH_2Cl_2, rt., overnight, 91% d) TFA in CH_2Cl_2, rt., 2h, 95% e) CH_3I in ACN, rt., overnight, 11%.

5.2.2.1 Methylation of the carboxylic acid of L-Cystine

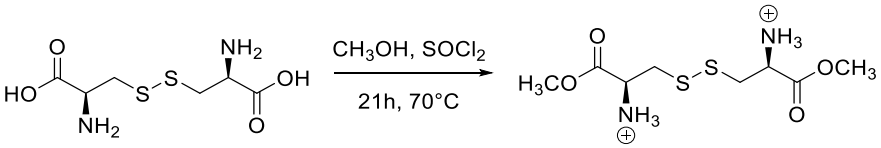

2.1

L-Cystine (21.82 mmol, 1 eq.) was dissolved in MeOH (80 mL). The solution was introduced into an ice bath and cooled at 0°C. Then, under N_2 atmosphere, $SOCl_2$ (110.35 mmol, 5.3 eq.) was added dropwise to the mixture using a needle and refluxed for 21 hours at 70°C. After that time, the MeOH was concentrated in the rotary evaporator and it was left to dry under vacuum for a few minutes. Finally, it was washed twice with diethyl ether (2 x 150 mL) and dried under vacuum overnight to remove the remaining diethyl ether.

Compound 2.1: (2S, 2'S)-3,3'-disulfanediylbis(1-methoxy-1-oxopropan-2-aminium)

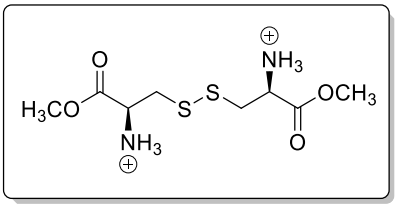

Yield: 99% (7.1 g, 20.81 mmol)

^{1}H-RMN (300 MHz, D_2O): δ 4.62 (dd, *J* = 6.6, 5.0 Hz, 1H), 3.91 (s, 3H), 3.55-3.30 (m, 2H).

5.2.2.2 N-protection of 6-aminohexanoic acid using Boc

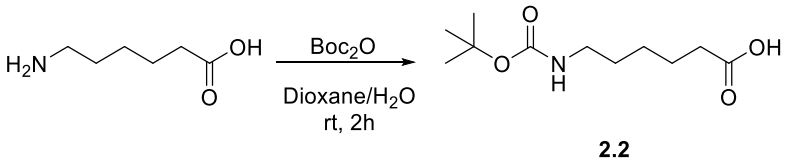

2.2

A mixture of dioxane/H_2O (200 mL/100 mL) was prepared to dissolve 6-aminohexanoic acid (38.12 mmol, 1 eq.). Then, the solution was introduced in an ice bath and cooled to 0°C. Following, 1M NaOH (38 mmol, 1 eq.) was added. Boc_2O (37.49 mmol, 1 eq.) was introduced five minutes later. The solution was stirred for 2h at room temperature. After that time, a stream of air was maintained overnight to evaporate the dioxane. After evaporating the dioxane, H_2O (50 mL) was added and the pH of the solution was adjusted to 4 with 1M HCl solution. The solution was extracted with ethyl acetate (2 x 50 mL) and the organic phase was washed with brine (150 mL). Next, it was dried with anhydrous sodium sulfate and filtered. Finally, the ethyl acetate was concentrated using a rotary evaporator and the product obtained was left to dry under vacuum overnight.

Compound 2.2: 6-((tert-butoxycarbonyl)amino)hexanoic acid

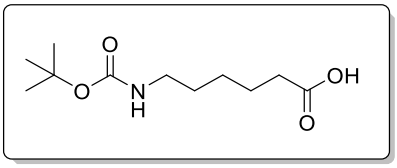

Yield: 82 % (1.45 g, 6.27 mmol)

^{1}H-RMN (300 MHz, $CDCl_3$): δ 3.10 (d, *J* = 5.9 Hz, 2H), 2.31 (m, 2H), 1.64 (m, 2H), 1.57-1.30 (m, 4H), 1.41 (m, 9H).

5.2.2.3 Coupling reaction between the derived molecule of L-cystine and the N-protected 6-aminohexanoic acid

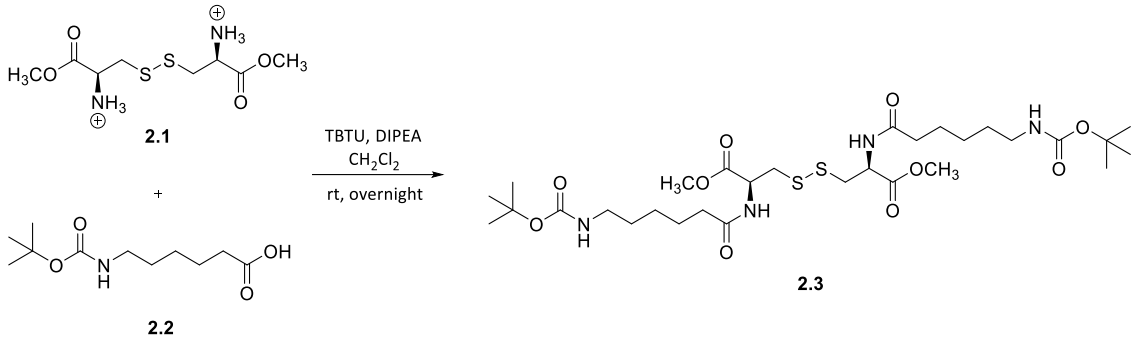

The compound **2.1** (13.57 mmol, 1 eq.) was dissolved in CH_2Cl_2 (50 mL). Under N_2 atmosphere, the compound **2.2** (27.14 mmol, 2 eq.) and DIPEA (56.98 mmol, 4.2 eq.) were added to solution. After a few minutes, TBTU (27.27 mmol, 2.01 eq.) was introduced into the solution. The mixture was stirred at room temperature overnight. The solvent was concentrated in rotary evaporator and the mixture was dried under vacuum to remove the remaining CH_2Cl_2. Next, the product was washed with basic water until a pH of 11 was reached to remove the remaining reagent and sonicated for a few minutes. After sonication, it was filtered through a porous plate. The filtrate was then washed again with acidic water until a pH between 3 and 4 was obtained to remove the remaining amine and sonicated again. The product was filtered again and finally wash was performed with water only to remove the excess of acid, repeating the previous procedure. The product was dried in the stove overnight.

Compound 2.3: Methyl (13S, 18S)-18-(6-((tert-butoxycarbonyl)amino)hexanamido)-13-(methoxycarbonyl)-2,2-dimethyl-4,11-dioxo-3-oxa-15,16-dithia-5,12-diazanonadecan-19-oate

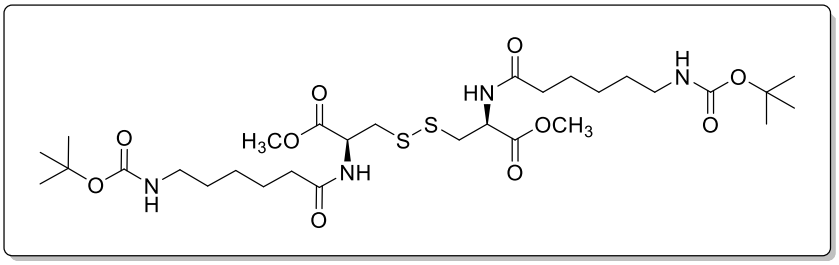

Yield: 91 % (8.43 g, 12.39 mmol)

^{1}H-RMN (400 MHz, DMSO-d_6): δ 8.31 (d, *J* =7.8 Hz, 1H), 6.70 (m, 1H), 4.54 (dd, *J* =13.4, 8.2 Hz, 1H), 3.64 (s, 3H), 3.11 (dd, *J* =13.7, 5.0 Hz, 1H), 3.00-2.79 (m, 3H), 2.10 (t, *J* =7.3 Hz, 2H), 1.48 (dd, *J* =14.6, 7.4 Hz, 2H), 1.35 (d, *J* =11.8 Hz, 11H), 1.22 (dd, *J* =14.2, 7.1 Hz, 2H).

5.2.2.3 Deprotection reaction of the Boc protecting group with TFA

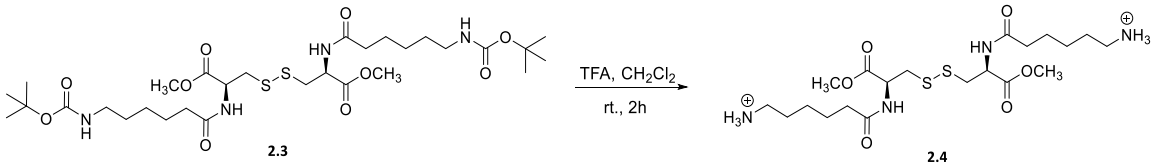

The compound **2.3** (1.47 mmol, 1 eq.) was dissolved in CH_2Cl_2 (11 mL) under N_2 atmosphere. Following, a mixture of TFA (49.83 mmol, 33.93 eq.) and CH_2Cl_2 (14.5 mL) was added dropwise to the reaction flask and it was stirred at room temperature 2h. After this time, the solvent was concentrated in the rotary evaporator. To elimate TFA residues, the mixture was washed with ether and concentrated on the rotary evaporator three times. The product obtained, oily appearance, was left to dry under vacuum overnight.

Compound 2.4: 6,6'-(((2S,2'S)-disulfanediylbis(3-methoxy-3-oxopropane-1,2-diyl))bis(azanediyl))bis(6-oxohexan-1-aminium)

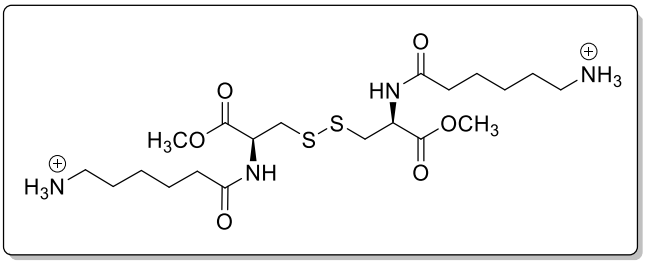

Yield: 95% (1.01 g, 1.40 mmol)

^{1}H-RMN (400 MHz, DMSO-d_6): δ 8.29 (dd, *J* =55.5, 7.8 Hz, 1H), 4.55 (dd, *J* =13.3, 8.3 Hz, 1H), 3.65 (s, 3H), 3.12 (dd, *J* =13.7, 5.0 Hz, 1H), 2.94 (dd, *J* =13.7, 9.0 Hz, 1H), 2.76 (dd, *J* =13.6, 6.6 Hz, 2H), 2.19-2.06 (m, 2H), 1.58-1.43 (m, 4H), 1.34-1.21 (m, 2H).

5.2.3 Experimental procedure for the synthesis of TriMeC$_6$CysHx

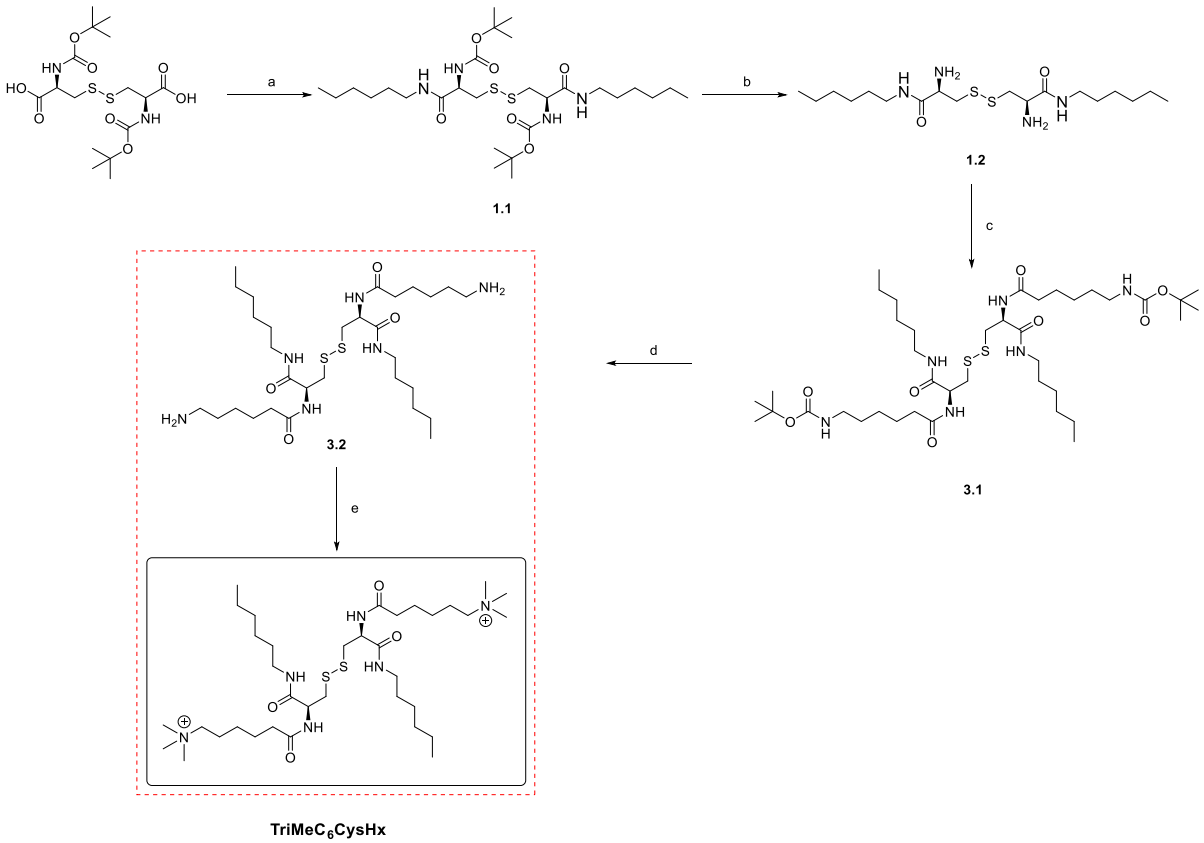

Scheme 5.3. Synthetic route 3. Reagents and conditions of: a) Hexylamine, TBTU, DIPEA in DMF, rt., 16h, 71% b) TFA in CH2Cl2, rt., 2h, then NaOH 81% c) 6-((tert-butoxycarbonyl)amino)hexanoic acid, TBTU, DIPEA in CH_2Cl_2, rt., overnight, 57% d) TFA in CH2Cl2, rt.,2h, then NaOH e) It was not carried out.

The first two intermediates of ***synthetic route 3*** (compounds **1.1** and **1.2**) are the same as those used in ***synthetic route 1***, so the experimental procedures followed to synthesize them are described in sections **5.2.1.1** and **5.2.1.2**, respectively.

5.2.3.1 Coupling between N-protected L-cystine and hexylamine

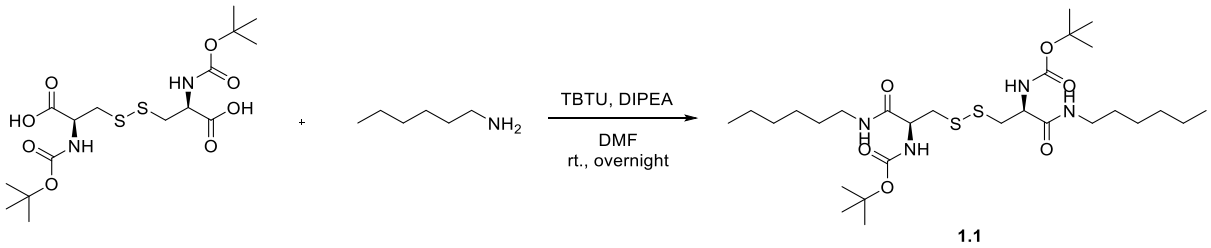

1.1

Experimental procedure and characterization using ^{1}H-RMN, ^{13}C-RMN and MS described in 5.2.1.1.

5.2.3.2 Removal of the Boc protecting group with TFA

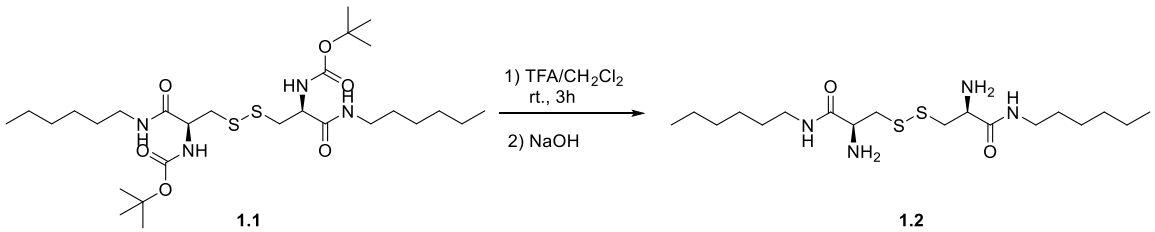

1.1 1.2

Experimental procedure and characterization using ^{1}H-RMN, ^{13}C-RMN and MS described in 5.2.1.2.

5.2.3.3 Coupling reaction between the derivative of L-cystine and the N-protected 6-aminohexanoic acid

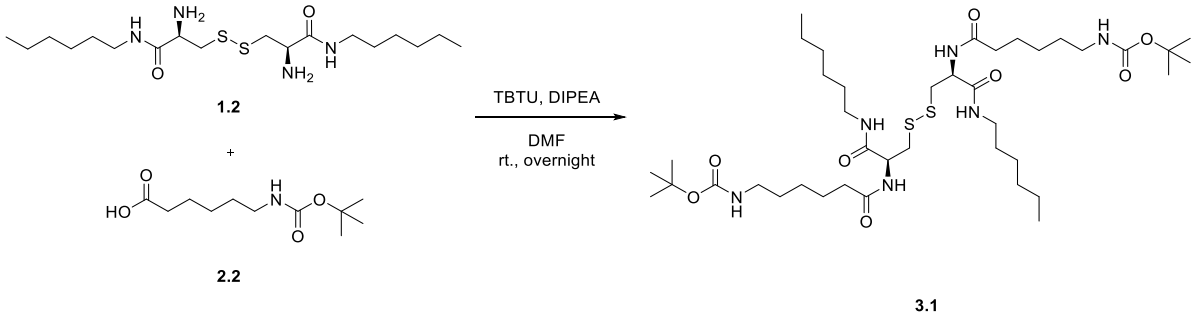

1.2 2.2 3.1

To a solution of compound **1.2** (5.31 mmol, 1 eq.) in DMF (100 mL), under a N_2 atmosphere and at room temperature, sequentially TBTU (10.72 mmol, 2.02 eq.), compound **2.2** (10.62 mmol, 2 eq.) and DIPEA (10.72 mmol, 2.02 eq.) were added. The resulting mixture was stirred at room temperature overnight. After this time, distilled water was added to the solution until a white precipitate appeared. The precipitate was filtered, washed with acidic water and sonicated for 20 minutes. After 20 minutes, it was filtered again, washed with basic water and sonicated another 20 minutes. Finally, it was filtered, washed with distilled water and sonicated for an additional 20 minutes. The solid was vacuum-dried overnight at 50°C.

Compound 3.1: di-tert-butyl ((((1R,1'R)-disulfanediylbis(2-hexylamino)-2-oxoethane-1,1-diyl))bis(azanediyl))bis(6-oxohexane-6,1-diyl))dicarbamate

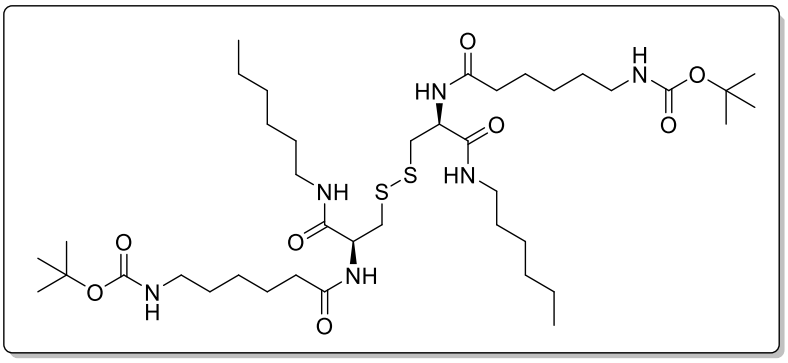

^{1}H-NMR (400 MHz, DMSO-d_6): δ 8.07 (d, *J* = 8.4 Hz, 1H), 7.93 (t, *J* = 5.3 Hz, 1H), 6.70 (s, 1H), 4.54 (dd, *J* = 14.0, 8.3 Hz, 1H), 3.14 – 2.95 (m, 3H), 2.85 (dt, *J* = 13.3, 7.6 Hz, 3H), 2.12 (t, *J* = 7.4 Hz, 2H), 1.56 – 1.11 (m, 24H), 0.85 (t, *J* = 6.4 Hz, 3H).

5.3 Preparation of nanoparticles

In a representative example, 300 µL of MPCysHx 50 mM in MeOH and 150 µL of Nile Red 200 µM in EtOH were added inside of snap cap clear glass vial. The vial was left in a vacuum oven at 50 ºC for 1 hour. Subsequently, 3.0 mL of distillate water was added (final concentration of MPCysHx = 5 mM; NR = 10 µM) and the mixture was sonicated for 10 minutes at room temperature.

Annex

6.1 NMR spectra

6.1.1 NMR spectra of *Synthetic Route 1*

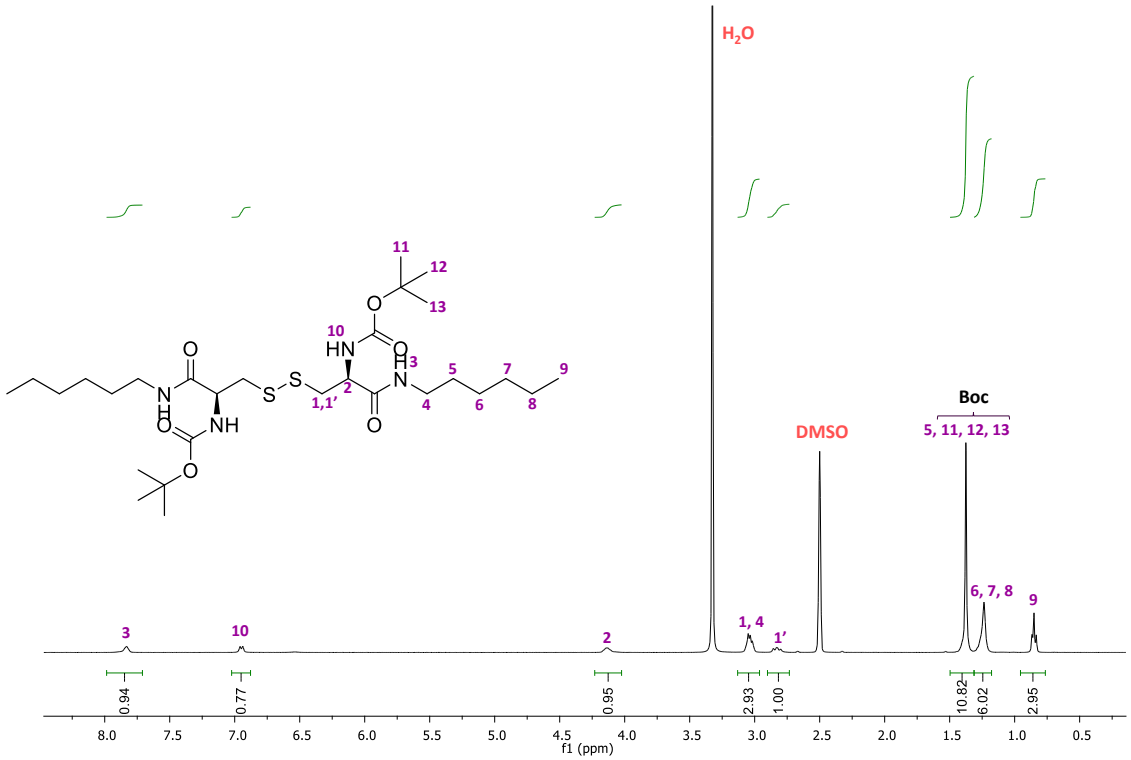

Figure 6.1: *^{1}H-NMR spectra of compound **1.1** in DMSO-d_6 at 400 MHz.*

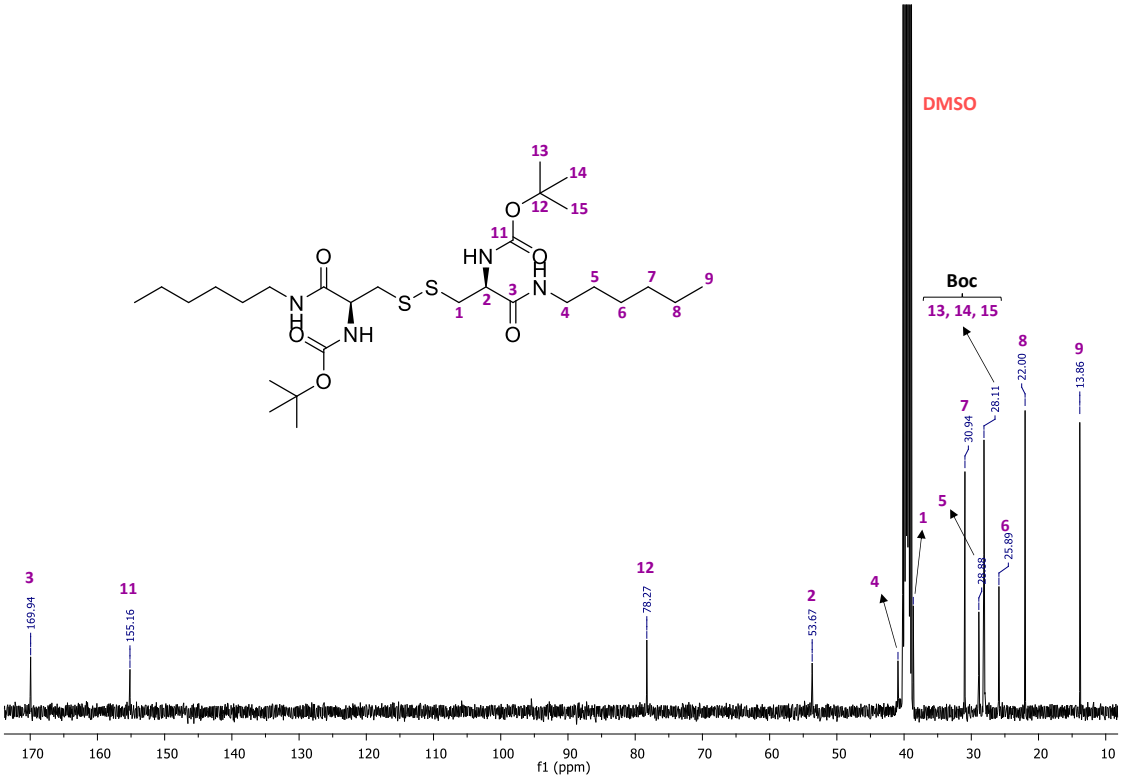

Figure 6.2: ^{13}C-NMR spectra of compound **1.1** in DMSO-d_6 at 101 MHz.

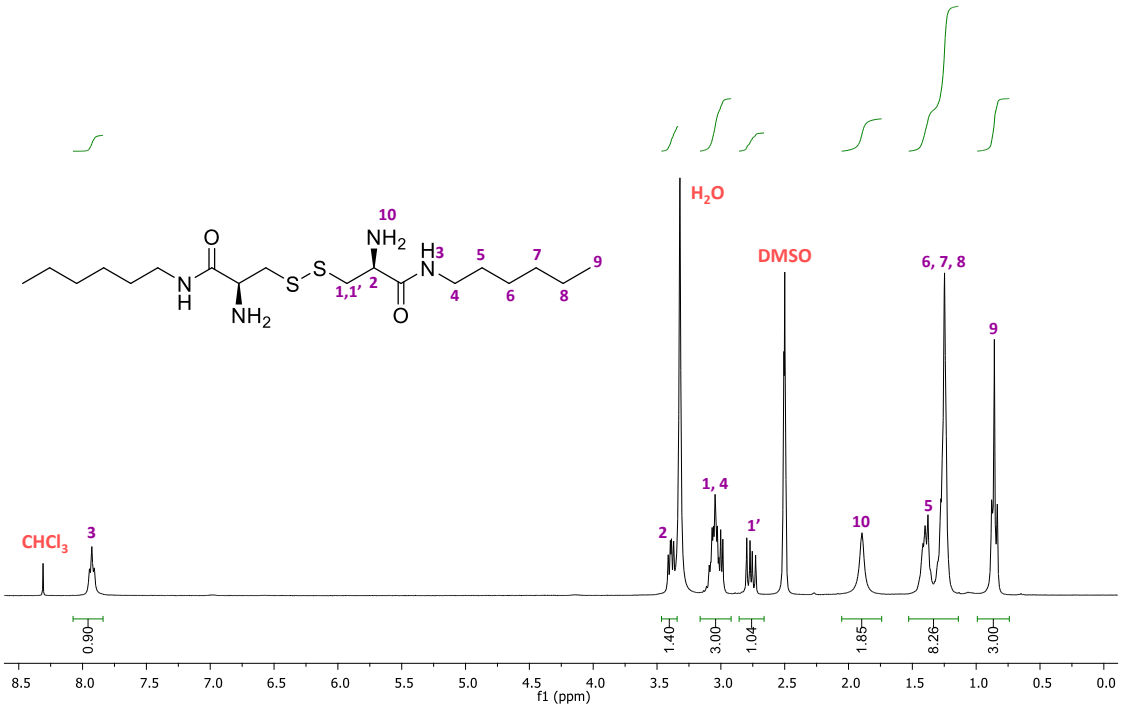

Figure 6.3: ^{1}H-NMR spectra of compound **1.2** in DMSO-d_6 at 300 MHz.

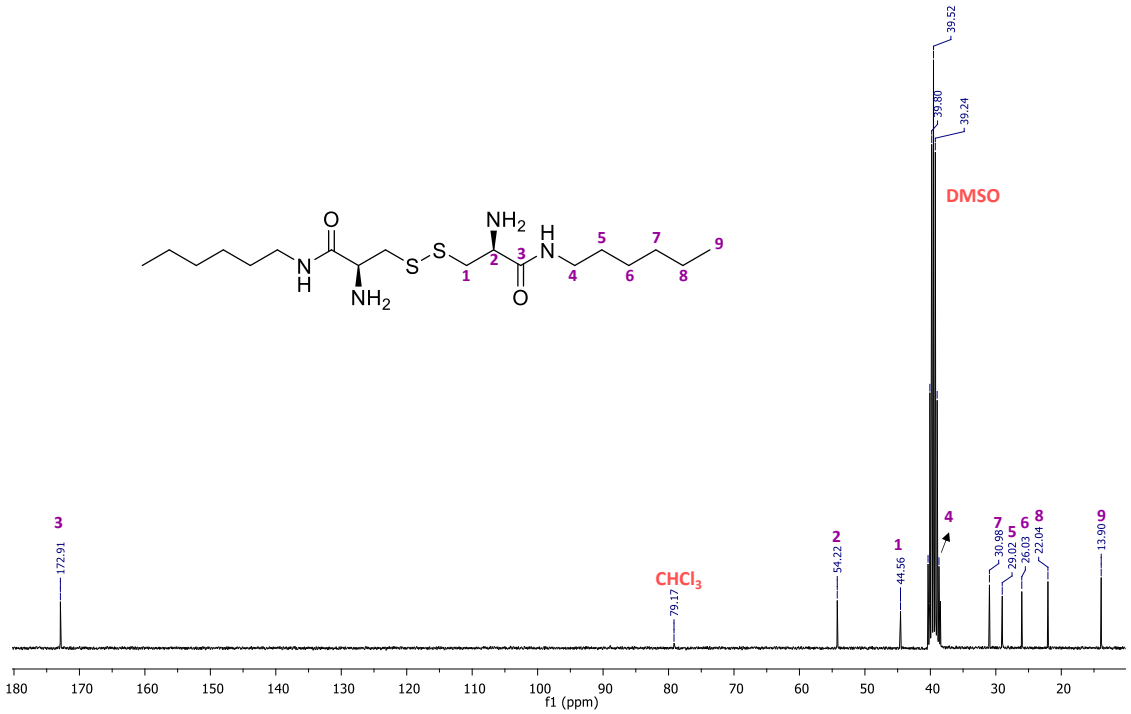

*Figure 6.4: ^{13}C-NMR spectra of compound **1.2** in DMSO-d_6 at 75 MHz.*

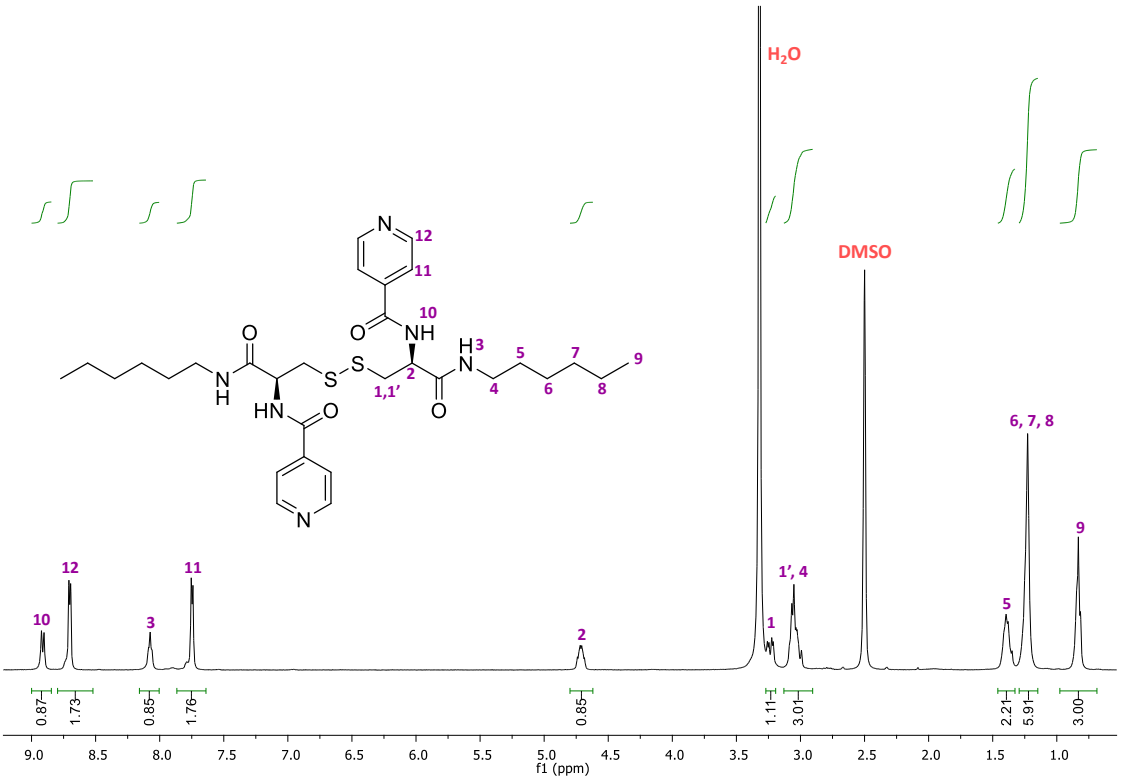

*Figure 6.5: ^{1}H-NMR spectra of compound **1.3** in DMSO-d_6 at 400 MHz.*

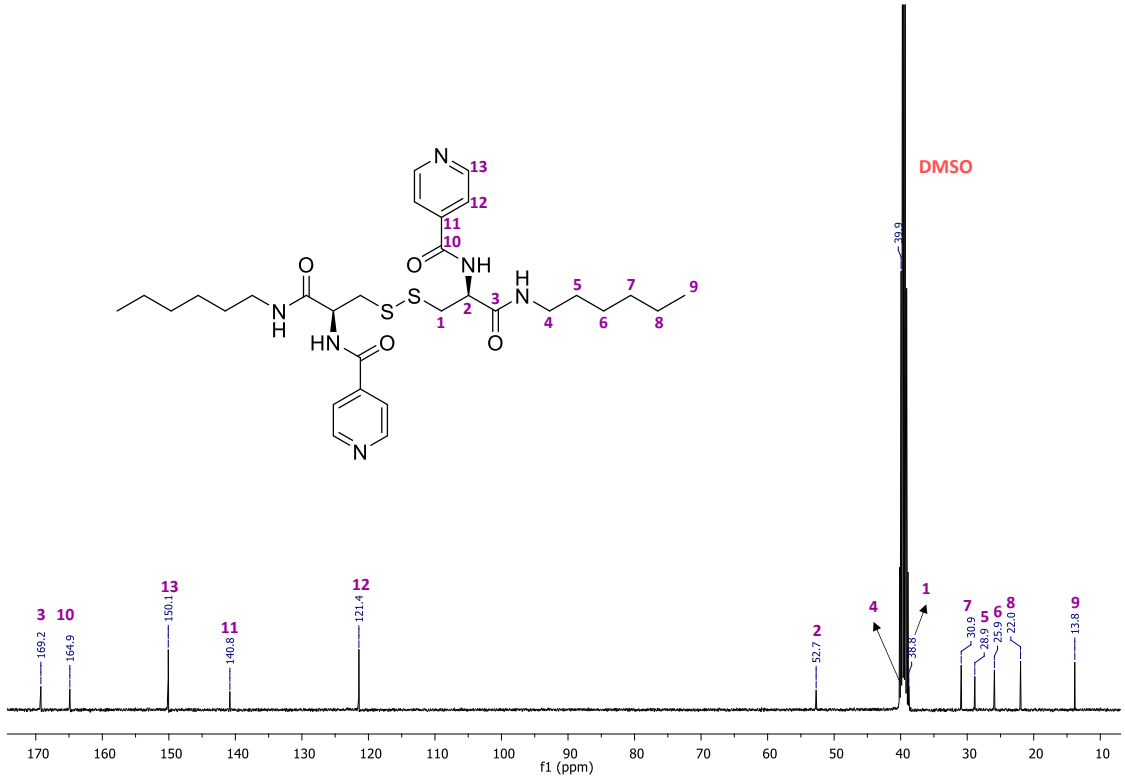

*Figure 6.6: ^{13}C-NMR spectra of compound **1.3** in DMSO-d_6 at 101 MHz.*

*Figure 6.7: ^{1}H-NMR spectra of **MPCysHx** in D_2O at 400 MHz.*

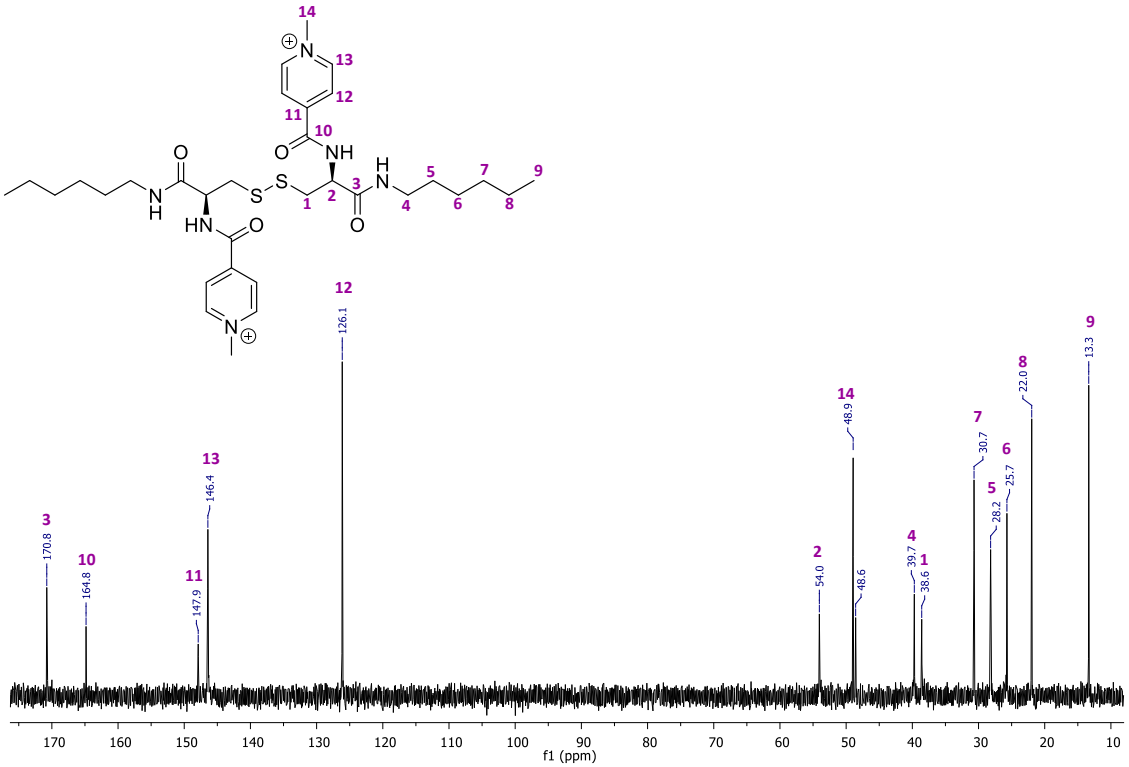

Figure 6.8: *^{13}C-NMR spectra of* ***MPCYsHx*** *in D_2O at 101 MHz.*

6.1.2 NMR spectra of *Synthetic Route 2*

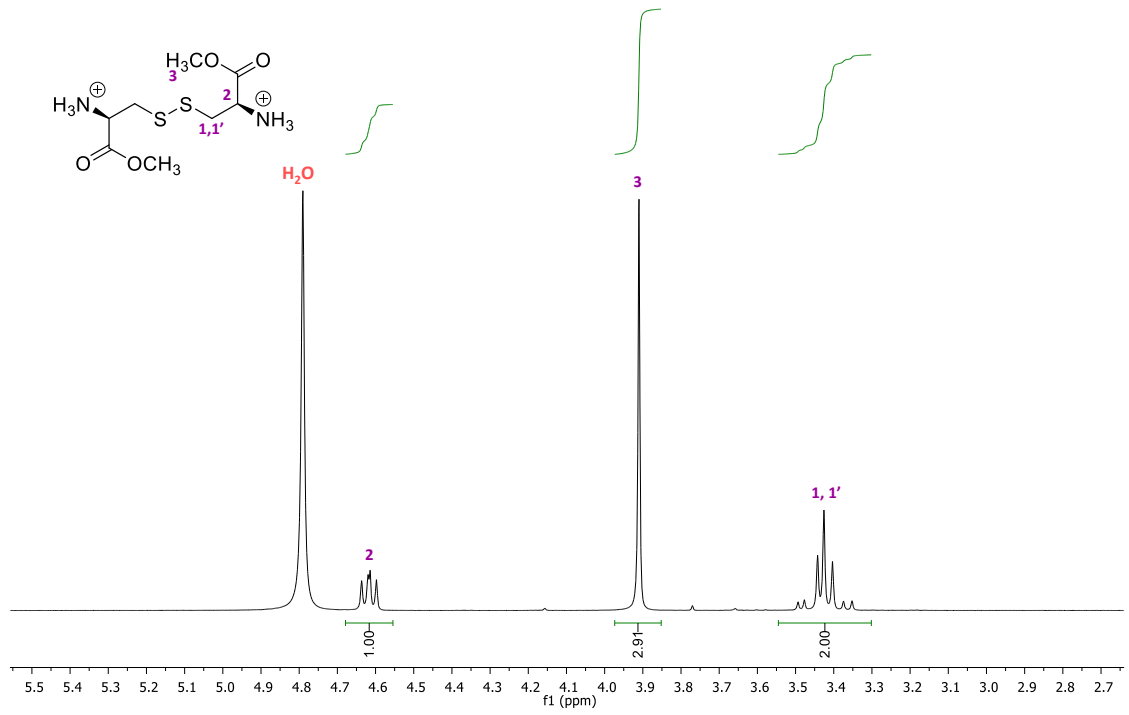

Figure 6.9: *^{1}H-NMR spectra of compound* ***2.1*** *in D_2O at 300 MHz.*

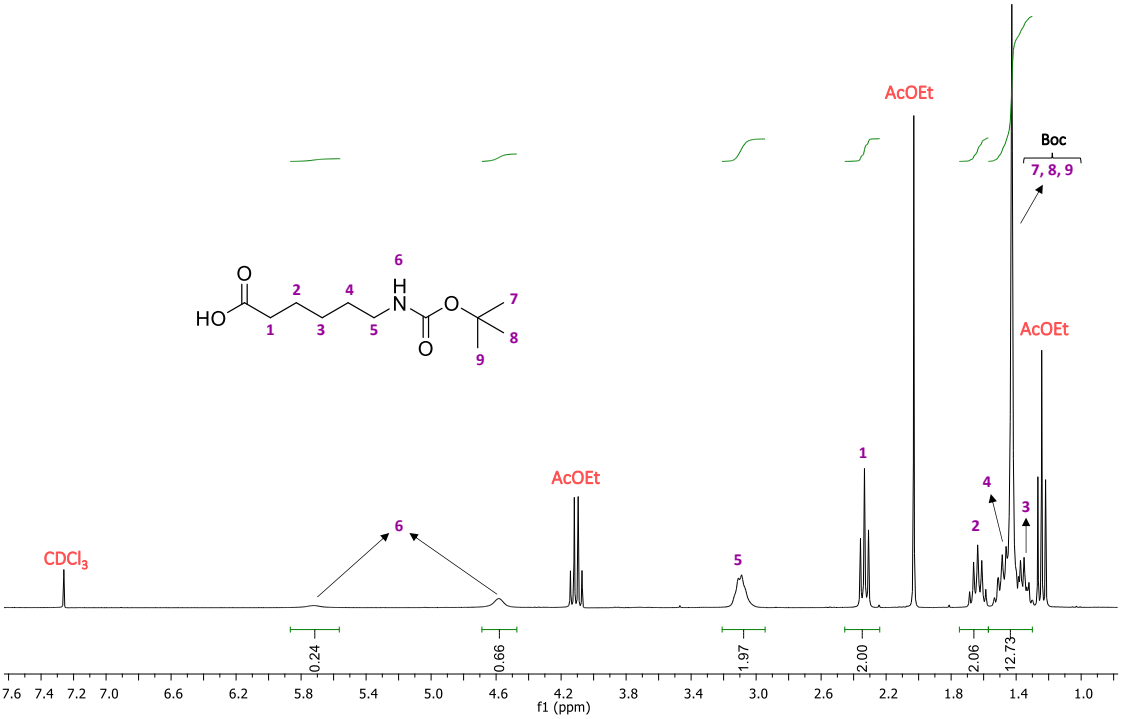

Figure 6.10: *^{1}H-NMR spectra of compound **2.2** in $CDCl_3$ at 300 MHz.*

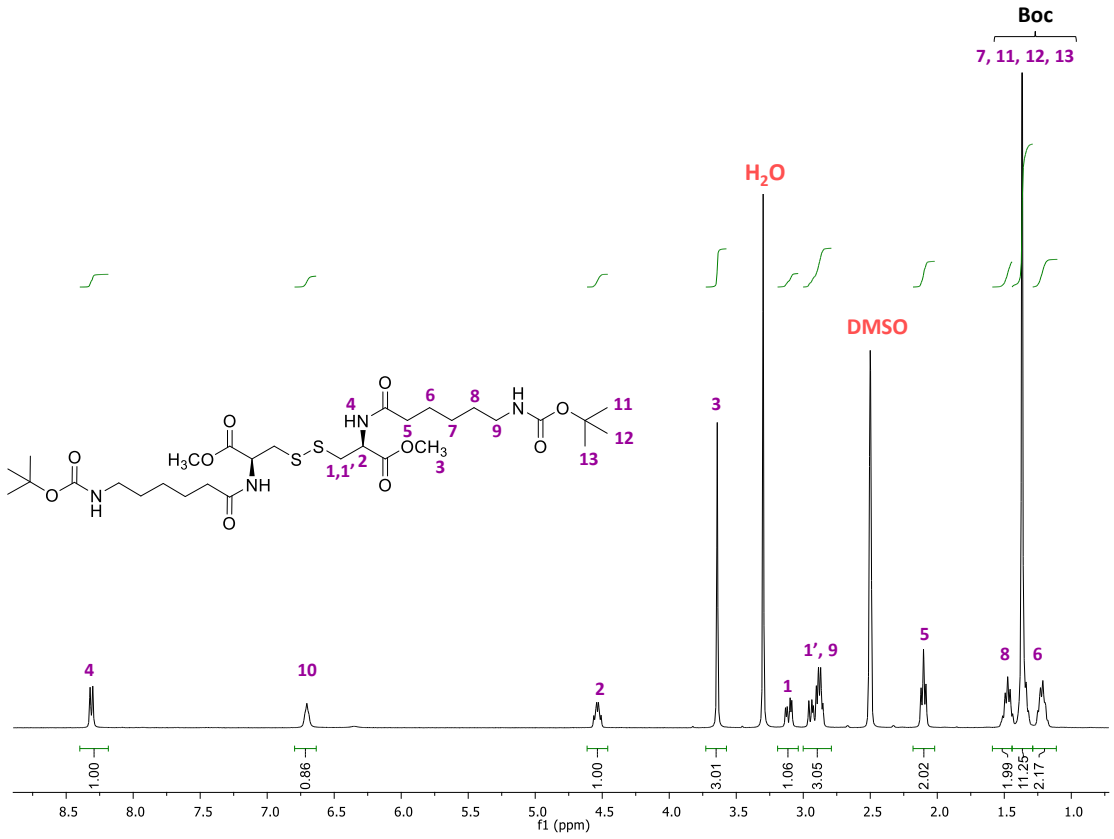

Figure 6.11: *^{1}H-NMR spectra of compound **2.3** in DMSO-d_6 at 400 MHz.*

6.1.3 NMR spectra of *Synthetic Route 3*

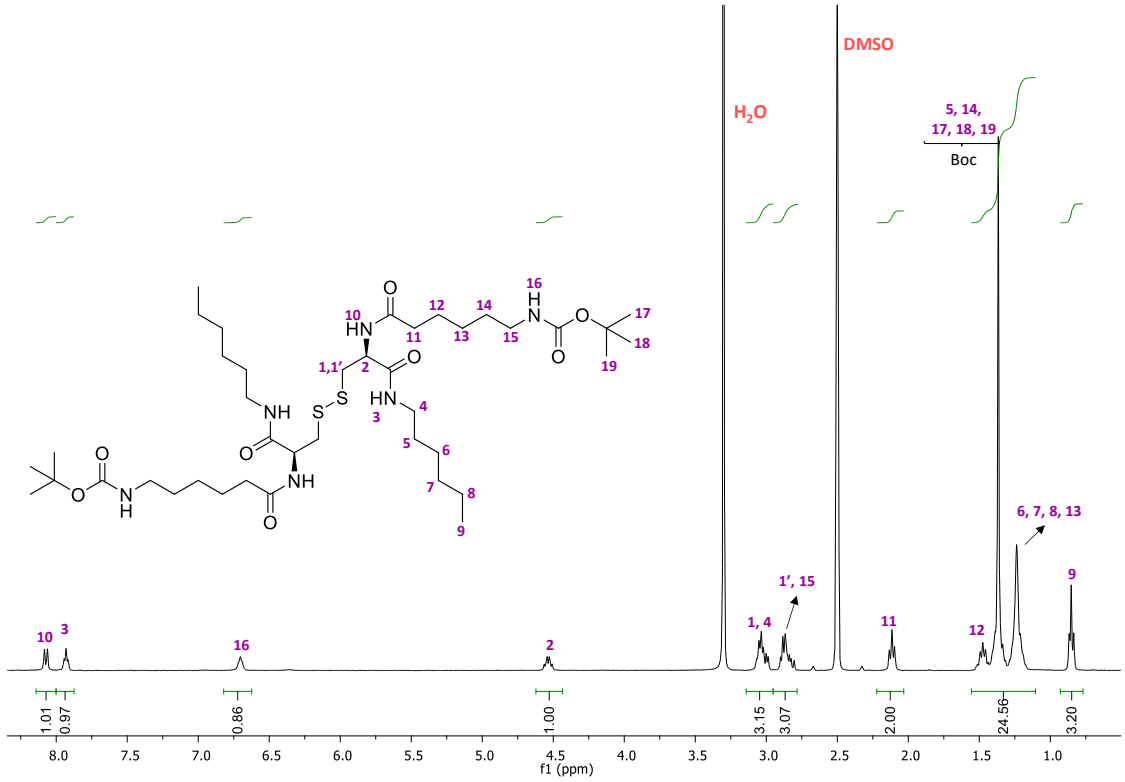

Figure 6.12: *^{1}H-NMR spectra of compound* ***3.1*** *in DMSO-d_6 at 400 MHz.*

6.2 MS spectra

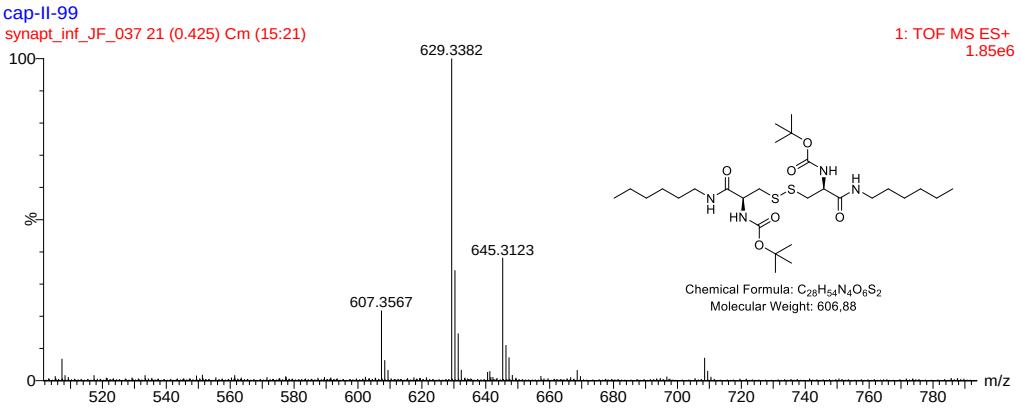

*Figure 6.13: MS spectra of compound **1.1**.*

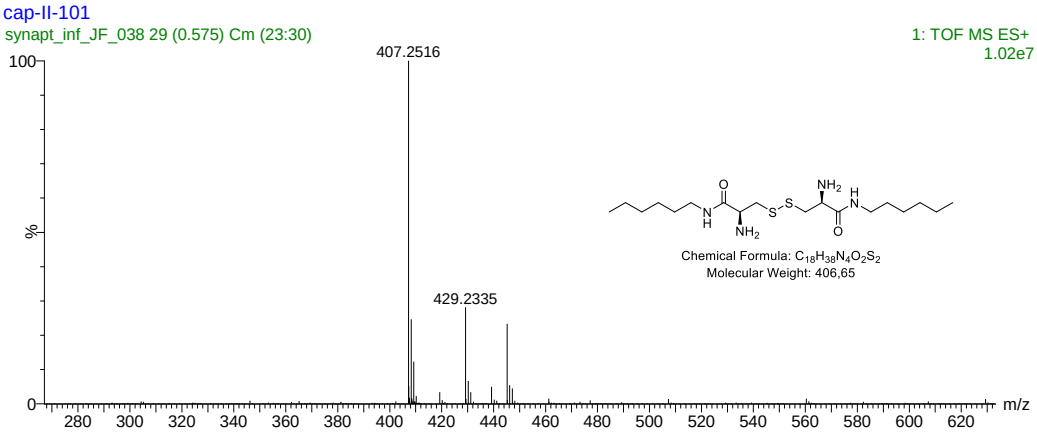

*Figure 6.14: MS spectra of compound **1.2**.*